

PROJECT FINAL REPORT

Grant Agreement number: 310250
Project acronym: UNION
Project title: Ultra-versatile Nanoparticle Integration into Organized Nanoclusters
Funding Scheme: Collaborative project
Period covered: from 01/02/2013 to 31/01/2016
Name of the scientific representative of the project's co-ordinator¹,
Title and Organisation: Dr. Dermot Brougham, School of Chemical Sciences, Dublin City University
Tel: +353 17005472
Fax: +353 17005503
E-mail: dermot.brougham@dcu.ie
Project website Fehler! Textmarke nicht definiert. **address:** <http://www.fp7-union.eu/>

¹ Usually the contact person of the coordinator as specified in Art. 8.1. of the Grant Agreement.

4.1 Final publishable summary report

(a) UNION Executive Summary

The European Union funded project 'Ultra-versatile Nanoparticle Integration into Organized Nanoclusters' (UNION), had the aim of developing nanoparticle (NP) assembly techniques, and assembly monitoring technologies to prepare novel hierarchically-ordered nanoparticle clusters (NPCs) at scale with controllable emergent properties for selected applications.

It is generally accepted that by improving control over the synthesis and assembly of nanoparticle building blocks it will be possible to produce materials with tailored and predictable properties. Furthermore, by incorporating hierarchical control into the assembly (through NP type, size and spatial distribution) it will be possible to improve performance and develop new functionalities.

In UNION the influence of order on properties was assessed and applications of NPCs in suspension (bio-medical), in 2D arrays (optical), and in 3D arrays or nanocomposites (thermoelectric, TE) were studied. The aims of the UNION project were the development of;

- (i) novel NP preparation methods;
- (ii) new insights into controlling assembly to produce hierarchical materials;
- (iii) platform technologies for assembling a range of NP types for multiple applications,
- (iv) new applications in process monitoring, drug-delivery, and thermoelectrics.

The project was divided into eight interconnected technical work packages (WPs). In WP1 novel NPs were prepared, reproducibly and at scale, with properties suitable for subsequent assembly, in WP2, into multi-functional nanoparticle clusters (NPCs) with compositional and dimensional hierarchy for each application. In WP3 the NPC and array formation processes were studied by building theoretical model of inter-particle interactions and through simulation of the assembly kinetics, allowing us to develop general rules applicable to a wider range of assembly processes. In WP4 the emergent functional properties (magnetic, optical, TE) of the NPCs were studied with a view to establishing tunable property control through the assembly process. In WP5 the bio-applications, in imaging and drug delivery, of hierarchical lipido-magnetic NPCs were developed. In WP6 we developed 2D arrays of optical NPs for sensing and lighting applications. In WP7 we developed 3D arrays of NPCs for TE applications. Finally in WP8 EHS, viability and scale-up to pre-commercial levels was undertaken for promising hierarchical assemblies.

A consortium of partners with expertise in NP synthesis, chemistry, physics, bio-applications, and a range of industries was built to achieve these goals. The Coordinator of UNION was DCU, Dublin where Dermot Brougham developed magnetic NPs and NPCs for MRI applications. LMU, Munich was responsible, among others, for the preparation of NPs and NPCs with optical functionalities and for overseeing the development of novel NPs (Jessica Rodríguez-Fernández), as well as for the simulation/computational aspects (Jacek Stolarczyk) that enabled application of selected NP assembly strategies to a range of NP types. From Fundacio Institut de Recerca en Energia de Catalunya (IREC), Barcelona, Andreu Cabot was responsible for managing the measurement of NPC properties, for developing thermoelectric nano-materials, and also was Quality Manager (designing/implementing QA across UNION). From MTA-EK, Budapest, Andras Deak was responsible for developing 2D NPC arrays. From Malvern Instruments Matthew Barea drove development of novel process monitoring technologies. Paolo Gasco (Nanovector, Torino) developed bio-applications of lipidomagnetic nanomaterials. German Noriega (Cidete, Barcelona) was Dissemination Manager and was responsible for developing of TE modules. Finally, Afshin Ziaei (Thales TRT, Paris) drove development of TE materials for a selected avionics application.

The outcomes of the project included a large library of novel NPs and NPCs with interesting properties, produced at scale using improved environmentally friendly processes that have been demonstrated to have reduced environmental impact over their life cycle and have undergone preliminary commercial assessment. In addition, 26 papers were published in high ranking journals (by project end). These partially encapsulate the significant contributions UNION have made to; (i) developing versatile bottom-up strategies based on assembly of NPs to produce consolidated nanostructured materials with improved performance; (ii) understanding the role of NP-NP interactions in forming monodisperse ordered clusters and classifying assembly processes.

(b) Summary description of UNION context and objectives

The key concept of the UNION project was to develop platform assembly techniques that can be applied to a range of NP types. Through innovation in NP synthesis and NPC preparation it was anticipated that UNION would be in an excellent position to gain new insights into controlling assembly to produce hierarchical materials and to investigate the effect of such hierarchy on the emergent properties of the assemblies. The goal was to use these capabilities to reproducibly prepare (at scale) nanocomposite materials that are beyond the state-of-art for multiple applications.

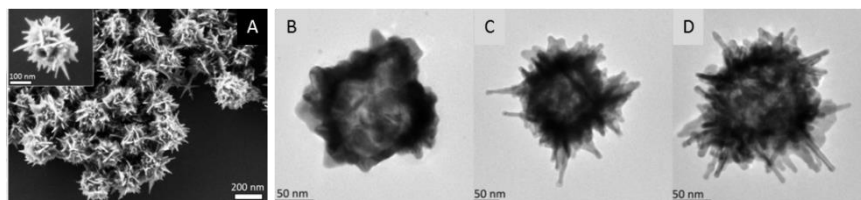
At the outset UNION our projected outputs included the development of:

- (i) novel NP preparation methods
- (ii) new insights into controlling assembly to produce hierarchical materials
- (iii) platform technologies for assembling a range of NP types, and hence multiple applications
- (iv) tested materials suitable for commercial development, for biological, process monitoring, and array (thermoelectric) applications.

- **Development / consolidation of novel nanostructured materials (NPs and NPCs).**

In the first period we developed a wide range of NP syntheses and NPC assembly methods, in the second period we improved and scaled-up the syntheses and characterised the materials performance more fully. This under-pinned the applications work (see below) and opened the way for 26 peer reviewed papers in international high impact journals (including *Nature Communications*, *ACS Nano*, *Small*, *JACS*, *Advanced Materials* etc.) to date, and with many more under review or in preparation. The range of materials prepared is too large to list fully here, however to select just a few examples from WP1 and WP2:

- A whole set of novel & high-quality NP building-blocks with improved optical-, magnetic-, TE- and bio-functionalities, and assembly potential, were obtained through improvements in



NP synthesis, surface chemistry and post-synthetic treatment. See for instance [“Simple and rapid high yield synthesis and size sorting of multi-branched hollow gold nanoparticles with highly-tunable NIR plasmon resonances”](#), Rodríguez-Fernández et al. *Small*, 2015, 11, 4550.”

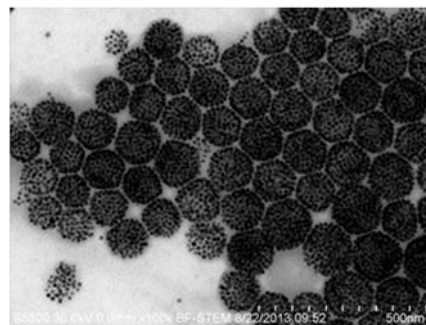
- Selected high-quality NPs were conveniently scaled-up, to the gram-scale in the case of thermoelectric NPs.
- The partners have aimed at more environmentally friendly, healthier and safer NP building-blocks when possible, and have taken into account the EHS assessment of the different NPs prepared. Alternative deployment of non-toxic, environmentally friendly and safer functional NP building-blocks was developed.
- For instance electrostatic assembly (ESA) was developed for metal-semiconductor hierarchical clusters of Au NR@Cu₂Se, by assembly of CdSe NPs on Au NRs followed by cation exchange, producing more environmentally-friendly NPCs with a unique and reversibly tunable plasmonic response. This work was published [“Switching plasmons: gold nanorod-copper chalcogenide core-shell nanoparticle clusters with selectable](#)

metal/semiconductor NIR plasmon resonances” Rodríguez-Fernández et al., J. Am. Chem. Soc. 2015, 137, 11666.”

- ESA was also applied to magnetic NPs, resulting in NPCs with interesting hyperthermic properties, and for assembly of TE NPs at scale.

- Polymer mediated assembly (PMA), in both the interface free and micellar collapse forms, was used to prepare NPCs from; (i) spherical and cubic magnetic (γ -Fe₂O₃) NPs, and; (ii) PbS (single NP component), PbS and PbSe (binary TE NP combinations).

- Competitive stabiliser desorption methods (CSD) were used to prepare single and multiple component monodisperse NPCs from γ -Fe₂O₃, CoFe₂O₄, MnFe₂O₄, and TiO₂ NPs reproducibly and at scale.



- Development of new insights into NP and NPC formation

By undertaking this activity the UNION partners developed new understanding of key processes at the nano-scale, and into the applications of the nanostructured materials. For instance:

- IREC and collaborators developed a simple and versatile bottom-up strategy based on the assembly of colloidal nanocrystals to produce consolidated yet nanostructured thermoelectric materials with improved performance. For instance, for the PbS–Ag system, Ag nanodomains contribute to block phonon propagation, reducing thermal conductivity, and also provide electrons to the PbS host semiconductor and reduce the PbS inter-grain energy barriers for charge transport, increasing electrical conductivity. Thus, PbS–Ag nanocomposites exhibit reduced thermal conductivities and higher charge carrier concentrations and mobilities than PbS nanomaterial. This work was recently published; *“High-performance thermoelectric nanocomposites from nanocrystal building blocks Kovalenko, Cabot et al. Nature Communications, 2016, 7, 10766”*

-DCU, MFA and LMU were invited by **Advanced Materials** to review the current state of the art in the use of colloidal methods to form NPCs. The manuscript *“Nanoparticle Clusters: Assembly and Control Over Internal Order, Current Capabilities, and Future Potential, Stolarczyk, Deak and Brougham” DOI: 10.1002/adma.201505350 was published recently.* In it we focused on the two-step approach (as in UNION) which exploits the advantages of bottom-up wet chemical NP synthesis procedures, with subsequent colloidal destabilization to trigger assembly in a controlled manner. The role of NP–NP interactions in the formation of monodisperse ordered clusters was pinpointed and the different assembly processes from a wide range of literature were classified according to the nature of the perturbation from the initial state.

- DCU and LMU have identified the key conditions that determine size control in thermal decomposition syntheses of magnetic iron-oxide NPs. This is an important area, with the original papers receiving >3000 citations in 10 years. The insights derive from application of accepted kinetic models, and provide clarity to the wide range of seemingly disparate published reports/observations. This work was described in detail at the Final Meeting, and it is now in preparation for publication in the ACS journal, Langmuir.

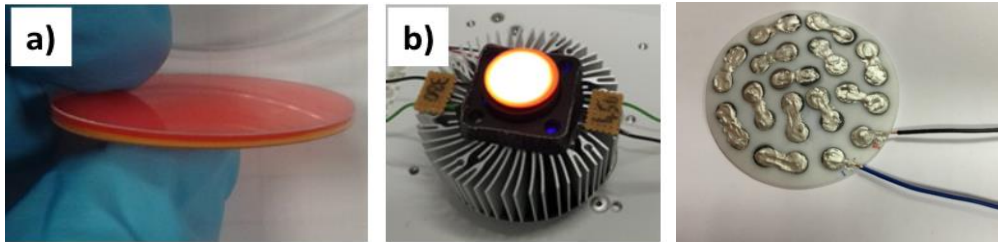
- Development of new Applications.

The objectives were to develop lipido-magnetic NPCs (DCU and Nanovector), nanostructured TE materials (IREC, Cidete and TRT) and process monitoring technologies (Malvern). This work was facilitated by the completion of the relevant (month 36) technical deliverables;

D5.5 and D8.2 “*Technology statement (for bio-application of selected NPC suspensions)*” including performance evaluation, EHS, LCA scale-up, estimated cost of production and market evaluation.

D8.3 “*Market assessment for TE 3D NPC array with obtained ZT values*”

D8.4 “*Economic viability and EHS of the production of 3D NPC arrays.....*”



and, by our internal and external scoping exercises;

D9.5 “*Industry workshops targeted at the biomedicine and thermoelectric energy market sectors, to promote collaboration and future market entry*”. Month 27.

D9.6 “*Roadmaps: Roadmaps for the targeted application areas to be developed by our SME/industry partners to prepare the future NPC commercialisation*”. Month 36.

At the end of the three year project the partners have made significant progress scientifically and towards each of the identified applications. We are now in a good position to develop these applications; towards alpha and the beta testing (for the assembly monitoring technologies), towards further patenting and sourcing in vivo testing (lipido-magnetic assemblies for bio-applications), and towards achieving a higher Technology Readiness Level, TRL (thermoelectrics – avionics).

For the assembly monitoring technologies the next steps will be completed in house and with partner laboratories, using available resources.

For the lipido-magnetic nanomaterials the next steps will involve identifying other sources of national project funding (this is underway) and the identification of industry partners with appropriate laboratory facilities for testing. Those contacts are being made.

For the thermoelectrics – avionics applications; higher TRL studies are envisaged through collaborative research projects integrating future supply chain actors. Additional partners are being sought to provide relevant end-user skills. A decision on how that work will be funded; be it through the resources of partners, or through external research funding, is currently under consideration.

(c) Description of the main S&T results/foregrounds from UNION

At the start of the UNION project our projected outputs were to develop:

- (i) novel NP preparation methods
- (ii) new insights into controlling assembly to produce hierarchical materials
- (iii) platform technologies for assembling a range of NP types, and hence multiple applications
- (iv) tested materials suitable for commercial development

In the last 36 months the consortium have made significant progress in this work. We developed robust nanoparticle synthesis methods for a wide range of NP types with control over size, shape, monodispersity, and ligand surface coverage. This allowed us to develop a range of NPC formation approaches suitable for different NP types and applications. Those innovations were consolidated through improvements in the processes, through process up-scaling, and through assessment of the materials from both environmental and life-cycle perspectives. By undertaking this activity the UNION partners developed new understanding of key processes at the nano-scale, and into the applications of the nanostructured materials. We have also progressed our identified technologies; lipido-magnetic NPCs (DCU and Nanovector); nanostructured TE materials (IREC, Cidete and TRT); and process monitoring technologies (Malvern); towards application. In the following sections the main S & T results from the project are summarised:

1. Production and development of functional NP building blocks.

UNION has produced a wide library of nanoparticles (NPs) with optical, magnetic, thermoelectric (TE) and bio-functionalities that have been used as building-blocks for nanoparticle cluster (NPC) formation (level-1 assembly) and 2D/3D array formation (level-2 assembly). By keeping in mind the functionalities and applications sought after in the project and the high-standards set in the Quality Assurance Plan (QAP), the partners have synthesized NPs of a wide range of materials displaying tailored size, shape, monodispersity, and surface chemistry. Environmental, Health, and Safety (EHS) aspects were also taken into consideration and actions were taken toward the utilization of safer and more environmentally-friendly materials.

In the following we describe a selection of representative NP building-blocks prepared across UNION attending to the four functionalities targeted. The examples selected represent important breakthroughs regarding functionality, morphology, surface chemistry, scale-up or EHS aspects.

(i) *Multi-branched and hollow gold (Au) NPs.* Within UNION, LMUM devised a simple and rapid strategy to synthesize multi-branched and hollow gold nanoparticles in a ~100% yield [A. J. Blanch, M. Döblinger, and J. Rodríguez-Fernández, “Simple and Rapid High Yield Synthesis and Size Sorting of Multi-branched Hollow Gold Nanoparticles with Highly-Tunable NIR Plasmon Resonances”, *Small* 11, 4550, 2015]. Representative electron microscopy images of the NPs are shown in Figure 1. They illustrate the control over branching extent and the hollow nature of these NPs. The combination of both features, branching and hollow interior is unique for NPs prepared by a seedless approach. Importantly, these NPs show strong plasmon resonances in the near-infrared (NIR) that are highly-tunable by adjusting their size, branching and hollowness.

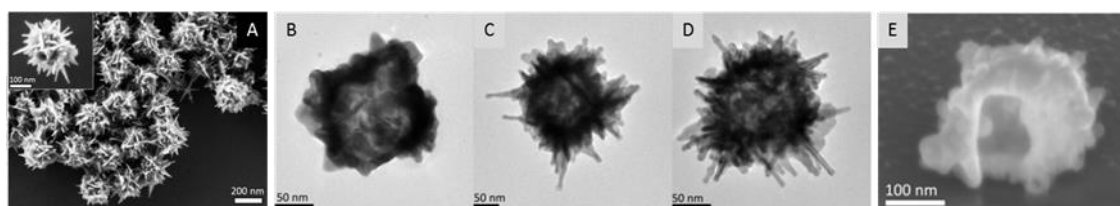


Figure 1. (A) Scanning electron microscopy (SEM) micrographs of a representative batch of multi-branched and hollow Au NPs. (B-D) Series of high-resolution transmission electron microscopy (HRTEM) images of individual

NPs obtained under different experimental conditions, and showing the control over NP branching. (E) SEM image of a NP milled with a focused ion beam. The image demonstrates the hollow nature of these NPs.

Investigations on the plasmonic performance of these NPs revealed: i) that even the non-branched nanoparticles show a very high plasmon sensitivity, *i.e.*, their plasmon resonance shifts strongly when the refractive index of the surrounding medium is changed, and this is due to their inherent hollowness; and (ii) that NPs with a high density of branches respond even more strongly (larger plasmon resonance shifts) to these refractive index changes, due to a high number of sharp tips *per* unit area. It was also demonstrated that a given colloidal dispersion of these NPs can be separated into highly monodisperse fractions (see Figure 2). This separation was achieved by centrifuging the corresponding colloidal dispersion in a centrifuge tube containing a glycerol density gradient. Importantly, the monodisperse fractions obtained can have plasmonic sensitivities higher than that of the original, unseparated, colloidal dispersion.

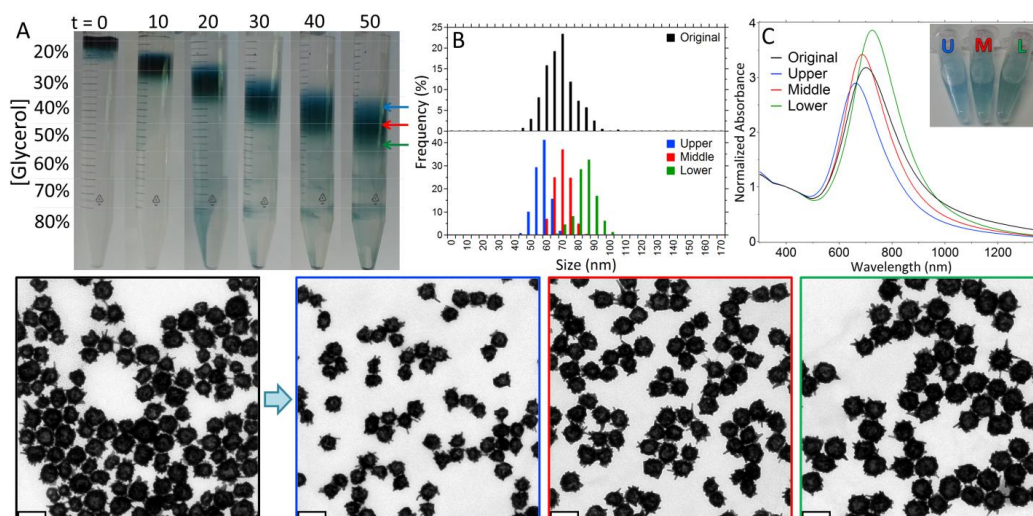


Figure 2. (A) Photograph illustrating the separation of a batch of multi-branched and hollow gold nanoparticles in a glycerol density gradient (2 mL steps) after centrifugation for 50 minutes. (B) Size distributions for the starting sample (top) and the for the upper, middle and lower fractions isolated (bottom). (C) UV-vis-NIR spectra for the same samples. The bottom row shows the TEM micrographs of the NPs in each sample.

(ii) *Patchy NPs.* Within UNION, MFA has prepared NPs with surface ‘patchiness’. ‘Patchy’ NPs, as understood here, have different stabilizers at different spots of their surface. This is quite important for controlling NP self-assembly, as depending on the interaction strength at those surface spots, different types of assemblies are possible. The demonstration of ‘patchiness’ was carried out on gold nanorods (Au NRs), see [Sz. Pothorszky, D. Zámbo, T. Deák, A. Deák, “Assembling patchy nanorods with spheres: limitations imposed by colloidal interactions”, *Nanoscale*, 2016, 8, 3523]. It was shown that under optimal conditions the cationic surfactant (CTAB, Au NR stabilizer) can be selectively replaced by cysteamine at the NRs’ tips (see step 1, Figure 3). In a second step, the CTAB left at the sides of the Au NRs was replaced by a thiol-ending polymer (polyethyleneglycol - mPEG-SH - see step 2, Figure 3). The effectiveness and selectivity of these surface modification steps was demonstrated by extinction and electrokinetic measurements.

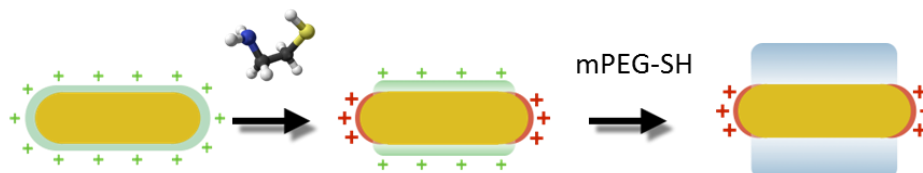


Figure 3. Scheme showing the formation of patchy Au NRs. Step 1: cysteamine replaces CTAB at the Au NRs’ tips. Step 2: mPEG-SH replaces the CTAB on the NRs’ sides.

(iii) *Functionalization of magnetic NPs with a wide library of assembly directors.* Within UNION, DCU has taken advantage of the surfactant free thermal decomposition method for NP synthesis (Pinna *et al.*, *Chem. Mater.*, 2005, 17, 3044). In this approach the solvent, here benzyl alcohol, in which the thermal decomposition takes place also acts as a weakly coordinating ligand, resulting in monodisperse NPs suspended in benzyl alcohol. Since the surface molecules can be easily displaced, the surface chemistry of the particles can be tuned according to requirements. This means that the type and surface density of the assembly directors (the final ligands) for Level-1 Assembly can be controlled. By varying the experimental parameters and with careful choice of workup it has proven possible to produce magnetic γ -Fe₂O₃ NPs of controlled size in 2 nm increments from 6 – 14 nm (with ca. 10% standard deviation in size), as shown in Figure 4.

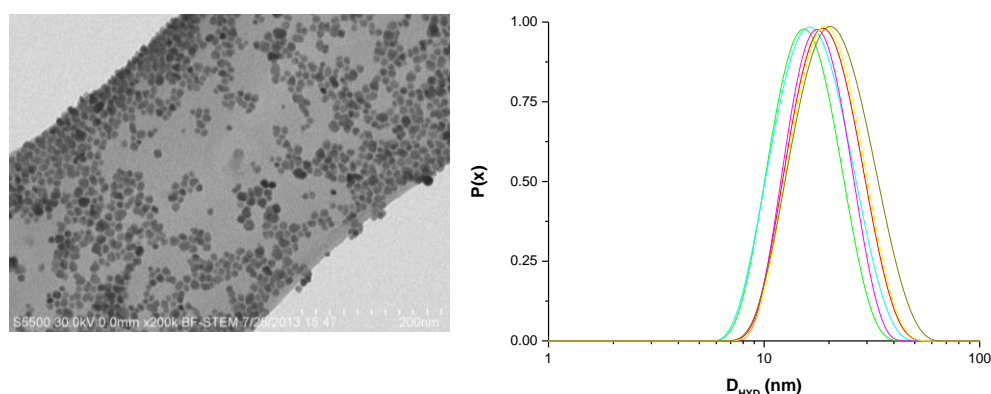


Figure 4 Left, TEM micrograph of oleic acid stabilised γ -Fe₂O₃ NPs synthesised using a 7 hour reflux and 16 g of precursor. Right, monotonic increase in hydrodynamic size distribution of suspensions in chloroform prepared with increasing quantities of precursor: (from the left) 0.66 g, 1 g, 2 g, 4 g, 8 g, 12 g and 16 g.

As shown, these magnetic γ -Fe₂O₃ NPs can be stabilized with a wide range of ligands (assembly directors). Among others, these include:

- Oleic acid, providing stable suspensions in CHCl₃ or heptane, suitable for CSD or PMA. The key point in this case is that the surface equivalent of OA can be tightly controlled, which is key for controlled Level 1 Assembly.
- Low molecular weight charged ligands, providing stable suspensions in H₂O, suitable for ESA. This has been demonstrated for (i) citrate, providing a high negative surface charge. A sample of this material will be sent to LMUM in the next week, (ii) dodecyltrimethylammonium bromide (DTAB), providing a high positive surface charge.
- Silanes, providing stable suspensions in H₂O. This has been demonstrated for: (i) (Aminopropyl)triethoxysilane (APTES), providing free amine groups suitable as a polymer initiator for grafting-from chemistries which were originally demonstrated by the DCU group for one NP size only [Brougham *et al.*, *Angew. Chem. Int. Ed.*, 2013, 52, 3164], (ii) (3-Glycidyloxypropyl)trimethoxysilane, providing free epoxy groups in high concentration as anchoring points for grafting-to chemistries [Brougham *et al* *Adv. Funct. Mater.*, 2011, 21, 4769].

(iv) *New solid lipid nanoparticle (SLN) formulation with improved drug retention.* Stearic acid SLN (SA SLN) with a small hydrodynamic size (d_{hyd}) and a low polydispersity index (PDI) were investigated due to their promising role as carriers for different applications (Piano *et. al.* *Eur J Neurosci*, 2013, 1853), most especially in ophthalmology, where earlier work has shown their capacity to deliver drugs to the back of the eyes. Within UNION, SA-SLN were synthesized by Nanovector through a patented microemulsion process. The main reason for this work was the

reported low stability of this type of NPs. By introducing key modifications to the formulation, it was possible to increase their physicochemical stability, drug loading capacity and retention over time.

For drug loading/retention testing, Myriocin (an amino fatty acid that inhibits serine palmitoyltransferase) was chosen as the model drug. Different strategies were tested for loading, including modification of; (i) the lipid composition; (ii) the lipid matrix/emulsifier ratio; (iii) the composition of the emulsifier layer. The best results were obtained by adding a new lipid component in the SLN matrix. These novel formulations showed reduced tendency to aggregate while maintaining low PDI (see Figure 5). Furthermore, the new lipid component also gave rise to a reduction in crystallinity that, in turn, is associated to an improved drug incorporation and retention over time (see Figure 6). The same drug release characteristics were maintained during performance of a simplified testing model (see Figure 6).

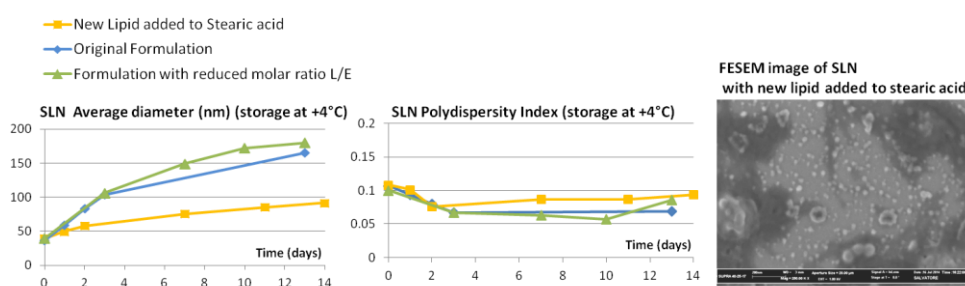


Figure 5 Physicochemical characterization of selected SA SLN samples as a function of storage time for the hydrodynamic size (left) and polydispersity index (right). Representative FESEM micrograph of the SLNs.

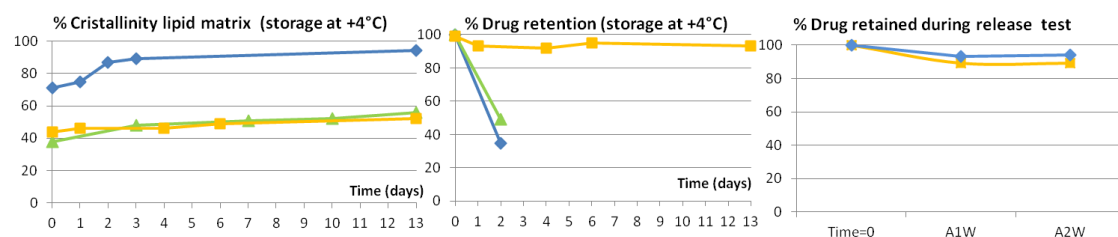


Figure 6: Comparative evolution of the crystallinity (left) and drug retention (center) of different SA SLN formulations upon storage at 4°C for 13 days. The corresponding drug release characteristics after one and two washing cycles are also shown (right).

(v) *Improvements over the doping and scale-up production of thermoelectric NP building-blocks.* Within UNION, IREC has demonstrated key advances on doping and up-scaling the synthesis of thermoelectric NPs.

Regarding doping, a novel approach was devised, where electronic doping was demonstrated by using surface ions [Journal of the American Chemical Society 2015, 137 (12), 4046-4049]. Halide ions were used as the basis for developing a new ligand removal procedure with three goals; i) removal of organic ligands from the NP surface; ii) introduction of assembly directors for the formation of NPCs and macroscopic nanocomposites; and iii) controlling the charge carrier concentration. As an example, HCl was demonstrated to provide a facile way to partially remove oleic acid from the NPs surface (Figure 7a), and at the same time dope PbS NPs. Chlorine is a common n-type dopant in bulk PbS. We believe that Cl⁻ remains at the PbS NP surface after oleic acid displacement, and from there it incorporates to the PbS anion sub-lattice during the nanocomposite consolidation step. The displacement of oleic acid by HCl was carried out by injecting controlled amounts of a 1.25 M HCl ethanol solution in 1 g of PbS NPs dissolved in chloroform. The mixture was stirred at room temperature in an argon filled glovebox for 1 h before purification by multiple precipitation/re-dispersion steps using anhydrous chloroform/methanol as a

solvent/non-solvent. For HCl amounts of up to 4.5%, PbS NPs remained soluble in relatively nonpolar solvents. TGA (Figure 7b) of the PbS NPs treated with different quantities of HCl clearly demonstrated the effectiveness of the HCl treatment for displacing OA from the NPs surface. As a reference, a PbS-0% sample, where oleic acid was displaced using NH_4SCN , was also produced. This sample was obtained using the procedure described in section 2.2. In a typical procedure, we mixed 6 mL of a 130 mM NH_4SCN solution in methanol with 1g of PbS NPs suspended in anhydrous chloroform. NPs were then purified using chloroform and methanol to remove free carboxylic acid and excess NH_4SCN , respectively. As in the second strategy, the charge introduced during the ligand displacement can be used to assemble the NPs into NPCs and macroscopic nanocomposites, which is the direction currently being pursued.

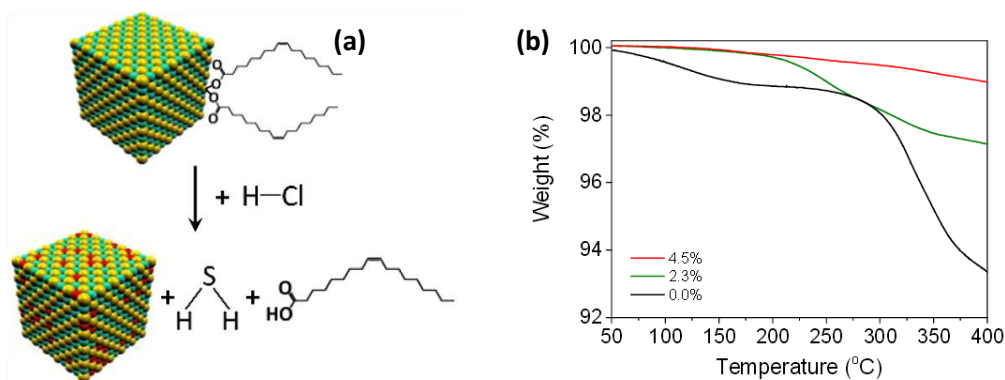


Figure 7. (a) Scheme of the HCl-based doping strategy. (b) Thermogravimetric profile of HCl treated PbS NPs.

Regarding up-scaling, IREC demonstrated the successful scale-up production of several thermoelectric NP building-blocks up to the gram scale, and identified critical scale-up aspects relating to each of them. Examples of selected NPs are shown in Figure 8. These results demonstrate the high quality, in terms of monodispersity and crystallinity of the NPs obtained.

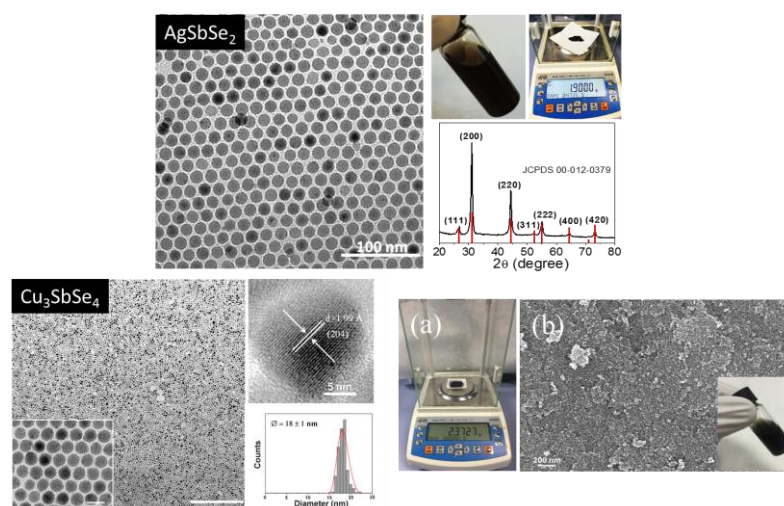


Figure 8. TEM, HRTEM, size distribution, and XRD patterns of selected NPs (top: AgSbSe_2 , bottom: Cu_3SbSe_4) as-obtained after up-scaling the syntheses to the gram scale.

(vi) *Actions towards the deployment of alternative NP building-blocks via $\text{Cd}^{2+}/\text{Cu}^+$ cation exchange reactions.* Cd-based chalcogenide nanoparticles are of high interest for applications spanning from lighting to solar cells. However, one of the drawbacks of such materials relates to the high toxicity of cadmium. Within UNION, LMUM has tried to overcome this issue by performing $\text{Cd}^{2+}/\text{Cu}^+$ cation exchange reactions on pre-formed Cd-based NPs. The potential benefits are three-fold:

1. From the EHS point of view, during the cation exchange process the highly toxic Cd^{2+} cations are replaced by less toxic Cu^+ ions.
2. From the morphological point of view the process only involves cation replacement, with the anion chalcogenide framework remaining unaltered during the process and therefore, with the morphology of the templating nanoparticles being preserved.
3. From the functional point of view, upon replacement of Cd^{2+} by Cu^+ , it is possible to obtain NPs with solely plasmonic properties (if the exchange is complete) or with excitonic and plasmonic (if the exchange is partial).

This way it is possible to exploit something negative from the EHS point of view, the presence of a highly toxic cation, to obtain identically-shaped nanoparticles with completely new optical properties upon replacement by a less toxic cation. Figure 9 illustrates the optical changes (from all-excitonic to all-plasmonic) occurring upon gradual cation exchange on pre-formed CdTe nanorods [Shedding Light on Vacancy-Doped Copper Chalcogenides: Shape-Controlled Synthesis, Optical Properties, and Modeling of Copper Telluride Nanocrystals with Near-Infrared Plasmon Resonances, I. Kriegel, J. Rodríguez-Fernández, J. Feldmann, et al ACS Nano, 2013, 7, 4367; and Cation exchange synthesis and optoelectronic properties of type II CdTe- Cu_{2-x}Te nano-heterostructures, I. Kriegel, J. Rodríguez-Fernández, J. Feldmann, et al, J. Mater. Chem. C, 2014, 2, 3189].

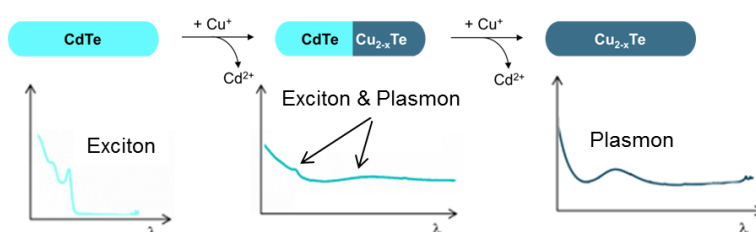


Figure 9. Sketch showing the evolution from CdTe NRs with excitonic properties, into CdTe- Cu_{2-x}Te heterostructured NRs with plasmonic and excitonic properties (partial cation exchange), and into Cu_{2-x}Te NRs with plasmonic properties (complete exchange).

2. Level 1 Assembly: Nanoparticle cluster Formation

(i) NP assembly by competitive stabiliser desorption, CSD

The DCU group developed the application of the CSD method for the production of single-component NPCs from magnetic $\gamma\text{-Fe}_2\text{O}_3$ or CoFe_2O_4 NPs. The NPC assembly process has now been fully optimised. [Brougham et al. *Journal of Materials Chemistry B*, 2015, 3, 8638 - 8643]. Briefly, we have now observed increased monodispersity of the suspensions, and excellent stability and reproducibility. The process has been scaled up by a factor of 12 and the materials have been phase transferred into water for application. In Figure 10 below the evolution of the suspension with time is shown. Note the increase monodispersity up to 20 hr (c.200 nm). In Figure 10 the cluster size analysis is also presented.

In more recent work the process was extended to TiO_2 NPs, and to the formation of multi-component hierarchical NPCs comprising multiple NP types. Finally the substrate used has been improved so that the process is more stable and cost-effective. That work has not yet been published so is not described in detail here.

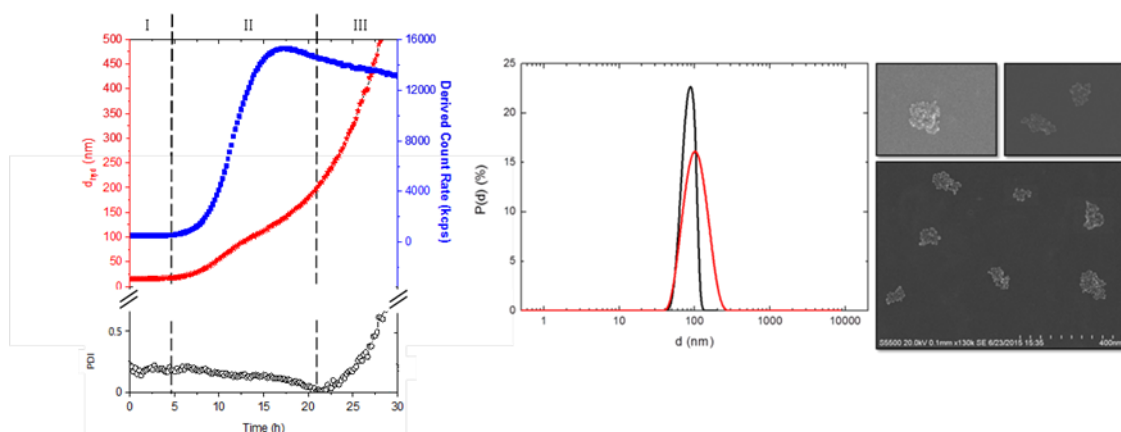


Figure 10. (Left) A typical NP assembly experiment at 1.2 mL scale in CHCl_3 , continuously monitored by DLS, which shows three stages evident from the evolution of the PDI value. Upper, time evolution of d_{hyd} (♦) following exposure to the silica substrate at $t=0$, backscattered light intensity (■). Lower, polydispersity index (PDI) (○). Note the time axis is common for both plots. (Right) Overlay of the DLS number distribution (red) for a NPC suspension (d_{hyd} 98 nm, PDI 0.09) and distribution (black) from log-normal analysis of FE-SEM images, yielding $d_{\text{SEM}} 85 \pm 13$ nm (16% deviation for 112 clusters). Right; representative FE-SEM images of NPCs from the same suspension, the scale bar is common to all the images

(ii) NP assembly by polymer mediated approaches, PMA

For biomedical applications, IREC and DCU have been investigating micelle-assembly methods using amphiphilic polymers (Pluronic F127 & P123). NPCs were formed using magnetic iron oxide (Fe_3O_4) NPs. The method is facile and the resulting NPCs are spherical and well-formed, Figure 11, and the cluster size can be controlled through the reaction conditions, in the case of an interface-free approach to the assembly (by evaporation of the co-solvent THF in the presence of a suitable polymer). The biocompatibility of pluronic compounds makes these methods especially advantageous for biomedical applications. By annealing the initial Fe_3O_4 nanoparticles in air at 120°C for 30 min to 1 hour after synthesis we can greatly enhance their magnetic properties. By using those nanoparticles and by utilizing a magnetic field on the micelle solution during the assembly, the resulting spherical NPCs are greatly improved and lattice alignment of the nanoparticles within the cluster is observed.

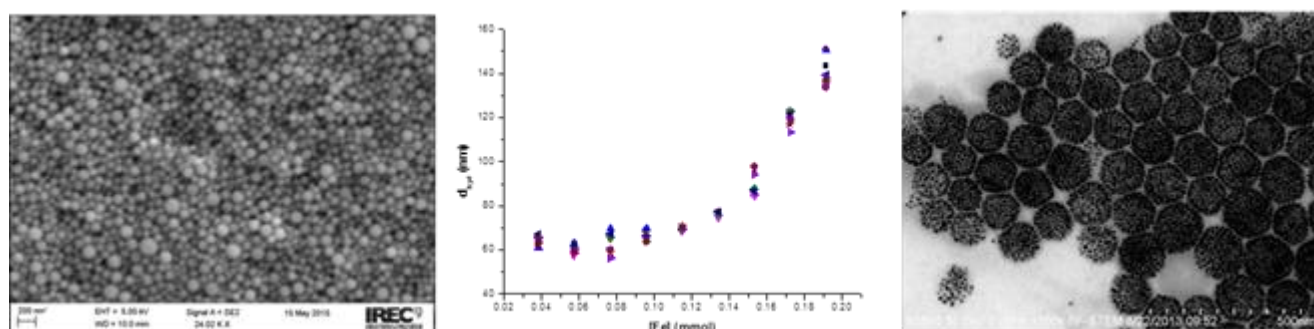


Figure 11: (Left) SEM image of Fe_3O_4 NPCs produced using F127 Pluronic acid (micelle collapse PMA). (Center) Control over NPC size (interface-free PMA). FE-SEM image of Fe_3O_4 NPCs formed from cubic NPs (interface-free PMA) exhibiting excellent monodispersity.

IREC have also developed the PMA methods for NPC production for TE applications. For instance IP-PMA was used to co-assemble PbS NPs (7.2 nm) and PbSe NPs (11.2 nm) into binary NPCs utilizing DTAB as a surfactant. This resulted in Se deficient NPCs (Se:S ratio 0.22-0.26), which were relatively monodisperse (151 ± 35 nm, 23%), in a reaction that is scalable (x75) with respect the original procedure.

(iii) ESA: metal-semiconductor hierarchical NPCs - Au NRs@CdSe & Au NRs@Cu_{2-x}Se (x≥0). Within UNION, LMUM has prepared multicomponent metal-semiconductor NPCs [H. Muhammed, M. Döblinger, J. Rodríguez-Fernández, “Switching Plasmons: Gold Nanorod–Copper Chalcogenide Core–Shell Nanoparticle Clusters with Selectable Metal/Semiconductor NIR Plasmon Resonances”, *J. Am. Chem. Soc.* 2015, 137, 11666-11677]. Gold nanorods (Au NRs) of aspect ratio ~ 2.76 were first modified with a negatively charged polyelectrolyte (polystyrene sulfonate, PSS) in order to reverse their surface charge from highly positive, due to the CTAB bilayer, to highly negative. The PSS-modified Au NRs were used as scaffolds for the electrostatically-induced self-assembly of tiny CdSe NPs on their surface, as reported by Kotov *et al.* (Nature Nanotechnology 6, 580–587, 2011), see Figure 12. The thickness of the CdSe supraparticle shell could be easily controlled as a function of the reaction time and, hence, hierarchical AuNRs@CdSe clusters with cadmium chalcogenide shells of tailored thicknesses were obtained (see Figure 12).

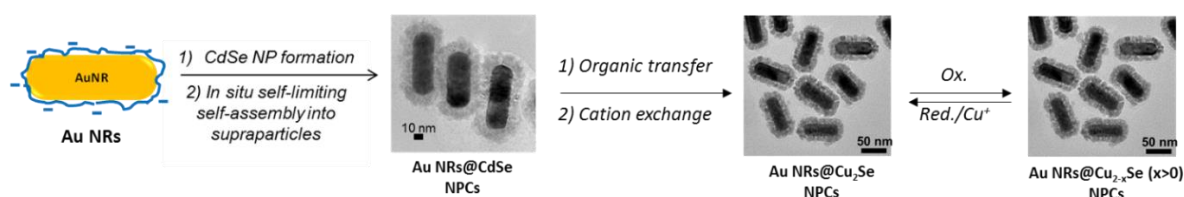


Figure 12. Scheme depicting the formation of multi-component metal-semiconductor NPCs (Au NRs@CdSe, Au NRs@Cu₂Se, and Au NRs@Cu_{2-x}Se) and the processes involved for the preparation of each.

In order to extend the library and functionalities of the metal-semiconductor hierarchical NPCs the know-how acquired on Cd²⁺/Cu⁺ cation exchange reactions on NPs [*ACS Nano*, 2013, 7, 4367; and *J. Mater. Chem. C*, 2014, 2, 3189, full refs given above] was extended to NPCs. For the preparation of more environmentally friendly Au NR@Cu₂Se NPCs, the Au NR@CdSe NPCs were first surface modified with octadecylamine to enable their redispersion into anhydrous toluene, the solvent where the cation exchange reaction is typically performed. Thereafter, cation exchange was carried out by addition of a Cu⁺ complex (see Figure 13). Elemental mapping confirmed the successful cation exchange, with the Au NRs@Cu₂Se NPCs consisting of Au NR cores and a supraparticle shell of Cu and Se (Figure 13). Importantly, these Au NRs@Cu₂Se NPCs can be converted into Au NRs@Cu_{2-x}Se (x>0) under oxidative conditions, and re-converted into Au NRs@Cu₂Se NPCs under reductive conditions, or in the presence of Cu⁺ ions (Figure 13).

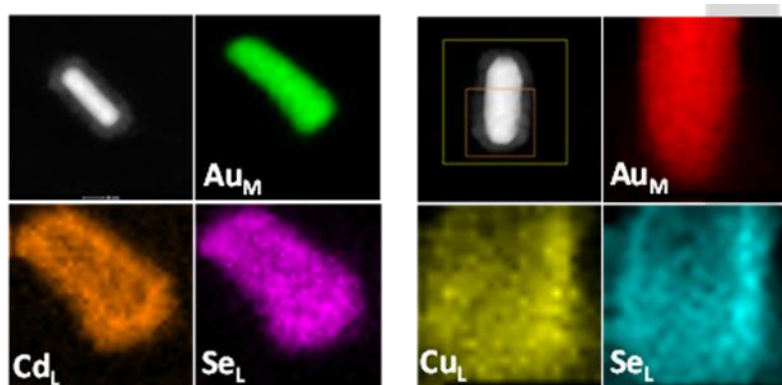


Figure 13. Representative EDX mapping of an Au NR@CdSe NPC (left) and of an Au NR@Cu₂Se (right), obtained after performing Cd²⁺/Cu⁺ cation exchange on the supraparticle CdSe shell.

Key information was obtained on the challenges associated with performing cation exchange on NPCs. Under optimal conditions (Cu⁺:Cd²⁺ ratios) the semiconductor NPs do not disassemble, *i.e.*, the shell is kept intact during the process. However, if the amount of Cu⁺ ions added is too high, disassembly occurs (see Figure 14).

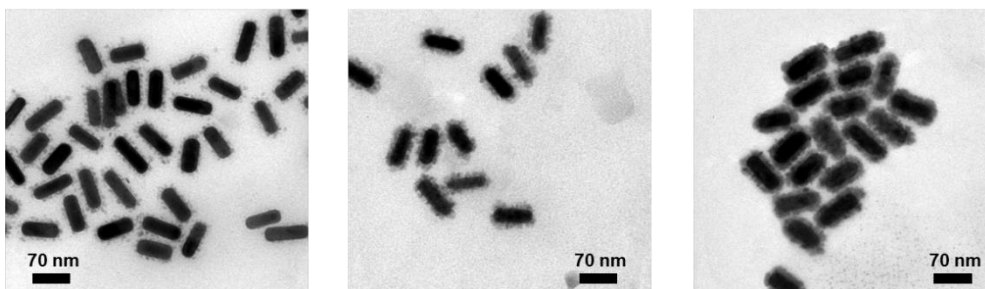


Figure 14. TEM micrographs of Au NR@Cu₂Se obtained by Cd²⁺/Cu⁺ on pre-formed Au NR@CdSe. In each case, the Cu⁺:Cd²⁺ ratios used are 6:1 (left), 4:1 (centre), and 2:1 (right). In the first two cases the process results in the disassembly of the newly formed Cu₂Se supraparticles. However, at lower ratios (right image) disassembly is prevented.

(iv) Assembly process monitoring. Malvern have completed the development of the DLS sizing probe which has subsequently been installed at DCU, Figure 15, for assessment and feedback into further developments. Through collaboration with Malvern, DCU can now monitor the assembly process *in situ* and directly compare these results with those obtained using the Zetasizer. Initial results from the probe system have proven promising when comparing to the specification of the Malvern Zetasizer. Extensive testing was completed on latex, gold nanoparticle and BSA samples all of which were in specification over a range of concentrations. Upon installation of the probe system at DCU it provided results within specification for instrument variability when compared with the Zetasizer on site. Two more probe systems have now been produced which are due to be sent out to customer trial sites identified by Malvern.

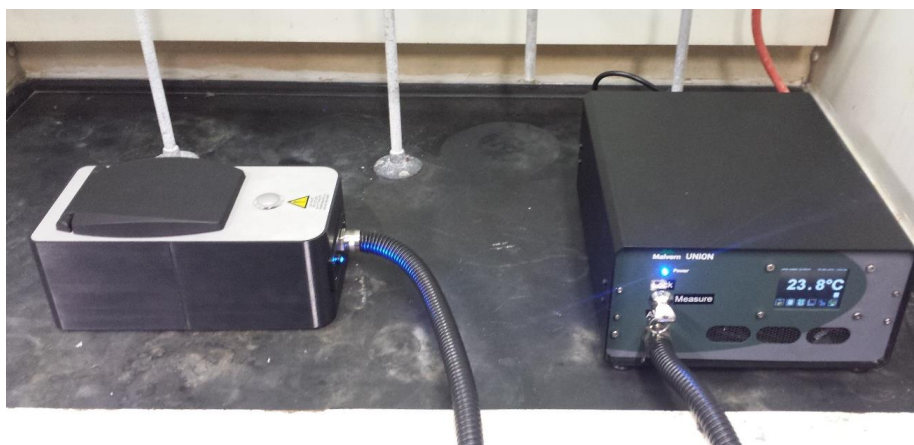


Figure 15. The final DLS prototype. On the left is the probe housed in a temporary enclosure (for protection/safety when not in use), with the remainder of the system housed on the right.

(v) Functional Assessment of NPCs (WP4) Note that a significant part of the UNION activity was to develop new materials properties, hence functional assessment of NPCs was a key activity (see WP4). For the purposes of this report we have included that activity in the relevant applications sections, below.

3. Cluster assembly monitoring and control (WP3)

Nanoparticle interactions The model of NP interactions was developed in order to understand the critical forces governing the assembly into NPCs. We also aimed to predict the optimal conditions for assembly and gain insights into the emergent properties of the clusters. The model included all relevant colloidal forces, i.e. van der Waals, magnetic, electrostatic and steric (osmotic, elastic, depletion) applied to the appropriate sizes of the NPs, where the range of interactions is often

comparable to the radius of curvature of the NP. The role of NP-NP interactions in directing the assembly under external perturbation (cf. Figure 16) into NPCs was extensively reviewed by DCU, LMUM and MFA [Stolarczyk, Deak, Brougham, *Adv. Mater.* **2016**, DOI: 10.1002/adma.201505350], as noted above.

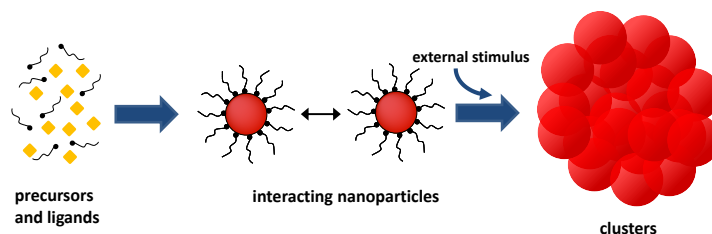


Figure 16: Illustration of assembly of pre-formed NPs determined by their interactions and induced by external stimulus.

The osmotic interaction was identified to often play critical role in the assembly, because modification of the ligand-solvent interactions can lead to reversion of the sign of the interactions so that it becomes attractive (hydrophobic interaction). For this reason we have extended the treatment of the osmotic NP-NP interaction to precisely evaluate it for very small NPs as wells for NPs coated with diffuse ligand layer (i.e. polymer layer with non-uniform thickness). We have applied the full model to a number of assembly scenarios. For instance we have shown that interactions of 8 nm iron oxide NPs are too weak to form a cluster which would be stable under addition of excess ligand (see Figure 17). On the contrary, NPCs made of 15nm NPs withstand such treatment. The calculations and the experiments on NPC assembled by CSD were in perfect agreement on that conclusion.

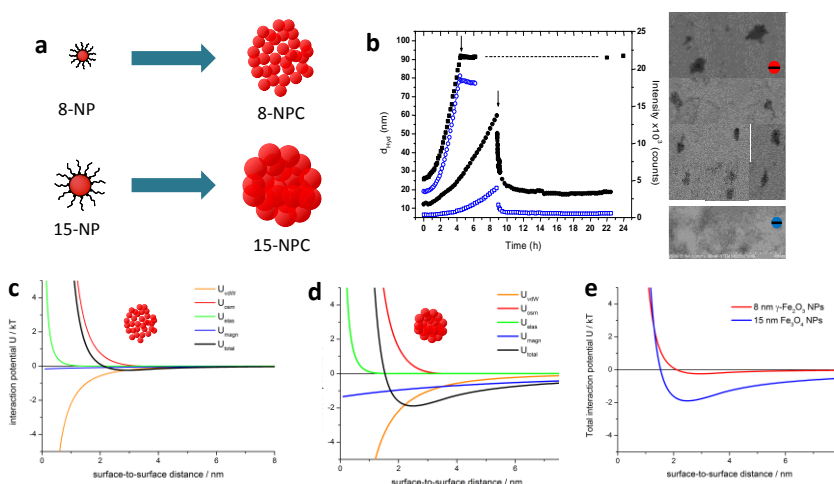


Figure 17: a) Schematic of assembly of NPs of different size into clusters; b) stability of NPC made of large NPs vs disaggregation of cluster made from small NPs; c) and d) interaction potential profiles of small and large NPs; e) comparison of interaction profiles.

The model was also applied to polyethylene glycol coated gold NPs. We have shown that a controlled collapse of the polymer shell through a change in salt content or temperature has led to an increase in van der Waals interactions and thereby into assembly into NPCs (see Figure 18). The experiments and calculations show that the strength of the interactions can be finely tuned by the experimental conditions of the process [Zambó *et al.*, *Langmuir* **2015**, *31*, 2662]. The model was used not only for spherical NPs, but also nanorods by MFA. Specifically, the predicted decoration

pattern of small charged NPs on the gold nanorods was found to be in agreement with experiments [Pothersky et al, *Nanoscale* **2016**, *8*, 3523-3529]

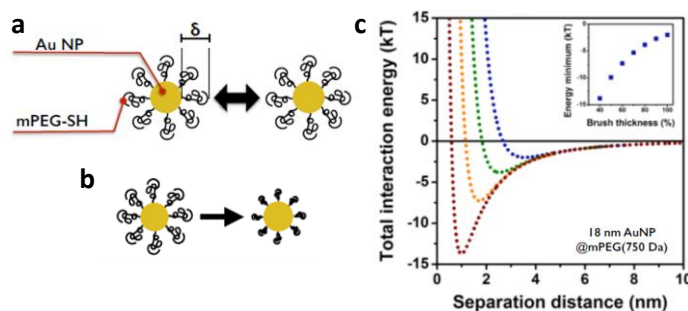


Figure 18: a) Illustration of interacting gold NPs coated with mPEG polymer brush; b) collapse/expansion of the brush depending on the salt content; c) interaction potentials as a function of the brush thickness.

The colloidal model has been shown to agree with experiments for NPs down to several nm in size. However, for smaller NPs several assumptions, e.g. the spherical character or uniform ligand distribution, are no longer accurate. In this context we have applied Density Functional Theory (DFT) calculations to evaluate the interactions between alkanethiol-stabilized ultra-small gold NPs. We have shown that indeed the effects of NP faceting and unique electronic configuration lead to different trends observed for such small NP than for their larger counterparts. Specifically, as seen in Figure 19, the interaction potential becomes stronger for NPs stabilized with longer ligands. Interestingly, this trend is not reproduced by colloidal theory calculations which do not account for the non-spherical shape of the NPs and the ligand-ligand interactions at the molecular level [Milowska, Stolarczyk, *Phys. Chem. Chem. Phys.* **2016**, DOI: 10.1039/C5CP06795B].

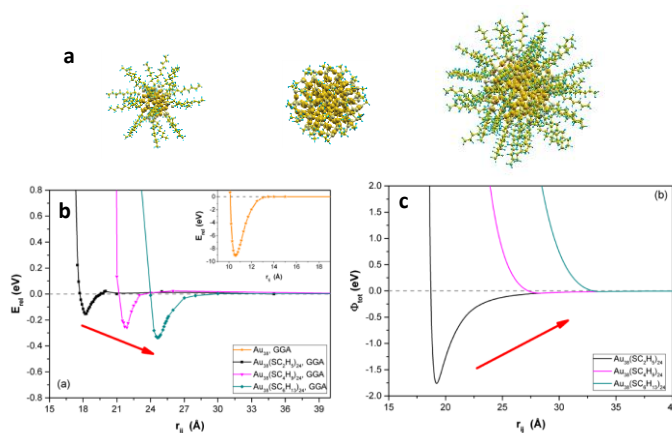


Figure 19: a) Sample alkanethiol-coated ultra-small Au NPs, studied by DFT methods; b) and c) Interaction profiles of Au NPs as a function of ligand length, calculated by DFT and colloidal stability theory.

Taking advantage of the periodic boundary conditions, the DFT calculations have been further implemented to calculate the preferential arrangement of the gold NPs in a cluster. In contrast to observations made for larger NPs which form body-centred cubic lattice, the ultra-small NPs were shown to form face-centred cubic lattice. This interesting computational result was confirmed by the HR-TEM and XRD analysis of the $Au_{144}(SC_6H_{13})_{60}$ NPs synthesized at LMUM and assembled into supracrystals. This provided for the first time insight into the formation of ultra-small Au NP assemblies both computationally and experimentally.

Arrays The interaction potential model was subsequently extended by MFA to NPC-NPC interactions in order to model NPC array formation. As described in detail in WP6 section, the

formation of arrays of gold NP rings by dewetting was controlled by the relative strength of NP-substrate, NP-NP and NPC-substrate interactions [Nagy et al, Identification of Dewetting Stages and Preparation of Single Chain Gold Nanoparticle Rings by Colloidal Lithography. *Langmuir* **2016**, *32* (4), 963–971]. It was found that while the NPC-NPC interactions were always repulsive, as needed for preventing uncontrolled assembly, the NPC-substrate needed to be reversed from attractive to repulsive to prevent random placement and enable the ring formation.

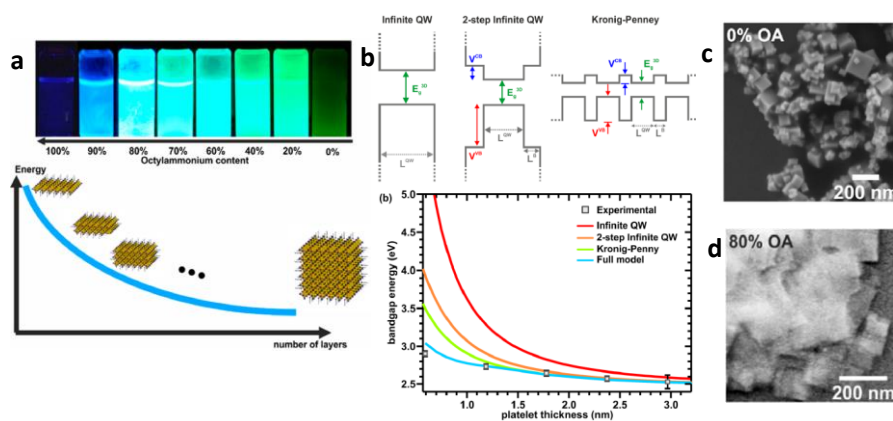


Figure 20: a) Comparison of photoluminescence of perovskite nanoplatelets as a function of long ligand content and the proposed structures; b) calculation of band gap on the basis of quantum confinement and exciton binding energy; c) and d) TEM images of the thick and thin, respectively, nanoplatelets.

We have also studied the thickness control and stacking behaviour of the organolead halide perovskite nanoplatelets. The material has recently taken the solar cell research by storm reaching 22% efficiency, but has been also suggested for LED applications. We have shown that by modifying the long vs short ligand ratio the thickness of the platelets and its tendency to stack can be controlled so that the emission wavelength can be tuned from green (for bulk or large cubic nanocrystals) to blue (for thin platelets), as shown in Figure 20. The calculations of quantum confinement and exciton binding energy in platelet stacks have allowed us to precisely determine the thickness of the platelets and explain the observed emission spectra [Sichert et al., *Nano Letters* **2015**, *15*, 6521-6527]. We have also shown that by controlling the osmotic interactions through solvent dilution the platelets can be fragmented providing additional level of control of the quantum confinements [Tong et al, *submitted*]. Carbon dots are another material exhibiting interesting emission properties in the blue-green range. We have studied the optoelectronic properties of the dots and their assemblies and have determined that the observed excitation dependent emission features are due to internal organization of the polycyclic aromatic chromophores rather than dot-dot or surface interactions [Fu et al., *Nano Lett.* **2015**, *15*, 6030-6035].

4. Nanoparticle clusters for bio-applications (WP5)

Iron oxide (γ -Fe₂O₃) NP and NPC suspensions in CHCl₃ were prepared by DCU for process development at Nanovector, i.e. coating with a lipid layer and subsequent phase transfer into water at physiological pH. The NPs and NPCs were formulated by the warm microemulsion (WME) method, previously developed by Nanovector to formulate solid lipid nanoparticles (SLN). Details of the composition cannot be disclosed here, however, we can describe the following nanomaterials.

Preparation of lipid stabilised dispersed magnetic nanoparticles (LNPs) with a thin conformal layer of lipids. LNPs could be used as targetable T₁-agents (local intensity enhancers) for magnetic resonance imaging (MRI). Such a thin lipid layer provides biocompatibility and colloidal stability, for targeting and for drug loading. However stability requirements and the need to retain the T₁ capability may limit the payload. See Figure 21.

Preparation of lipid stabilised clusters (LNPCs) which are lipid encapsulated clusters formed from pre-existing clusters (NPCs) of magnetic nanoparticles. Typically the NPCs are formed in a controlled fashion in a first step, e.g. by the CSD method, and are subsequently lipid encapsulated/phase transferred into aqueous media. Among the potential advantages of LNPC suspensions are that lipid encapsulation of preformed NPCs would allow for the optimisation of r_2 -relaxivity (efficacy for T_2 -weighted MRI) using cluster assembly approaches developed in UNION with potential subsequent inclusion of a drug payload **WITHIN** the biocompatible coating.

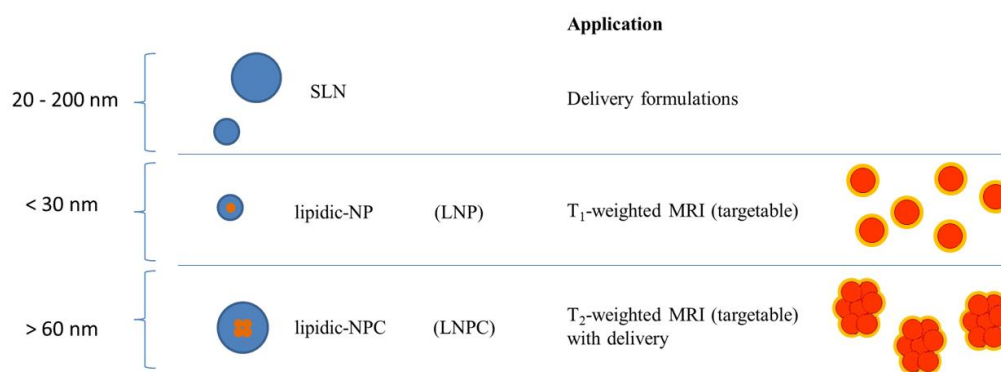


Figure 21. Schematic representation of the biocompatible lipidic and lipido-magnetic nano-materials developed in UNION. Note that solid lipid nanoparticles (SLN) are well-known drug carriers, for which Nanovector has background IP. LNP are single lipid-stabilised dispersed NPs in aqueous media. LNPCs are single lipid-stabilised clusters in aqueous media, formed from encapsulating pre-existing NPCs.

(a) LNP suspensions

The preparation of aqueous LNP suspensions (disperse particle stabilised by lipids, at physiological pH) following encapsulation of NP suspensions using developments of Nanovector's WME process was confirmed by Gel Filtration Chromatography (GFC) analysis Figure 22. As all lipid components showed the same elution trends, it was clear that the nominal formulation was retained in the final product when the optimised lipid formulation, and NP concentration are used. Furthermore, analysis confirmed reduced presence of clusters and of unloaded SLNs (NP free), see fractions 7, 8. These can be then purified by standard manufacture process techniques.

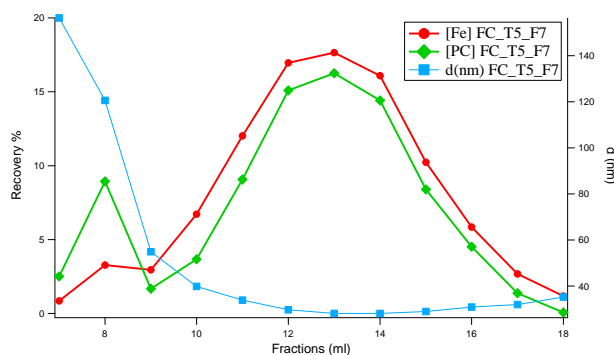


Figure 22. GPC profiles for LNP suspensions confirming the possibility of producing fully dispersed NP suspensions. PC content (green), Fe content (red) and d_{hyd} (blue).

(b) LNPC suspensions

NPC suspensions in CHCl_3 with d_{hyd} ranging from 60 to 200 nm, and low PDI typically <0.1 were prepared using the CSD process, by DCU. These were phase transferred by lipid encapsulation by Nanovector. In the optimised process it was possible to produce aqueous suspensions with a high yield of LNPs without significant change in cluster size or polydispersity. As temperature was shown to disaggregate the clusters, the WME process was adapted to room temperature, mainly by use of solvents. The resulting lipid coated LNPC suspensions were purified, and separated from small fraction of free SLN, and/or small LNPs by magnetic separation. LNPC formation was confirmed by DLS and GPC Figure 23. LNPC have an average mole ratio, PC/Fe, of $c.2.5\%$. For LNP suspensions the PC/Fe value was $c.5\%$. This suggests similar surface coating for both types, with the expected reduction in lipid content given the reduced relative outer surface area of the LNPCs.

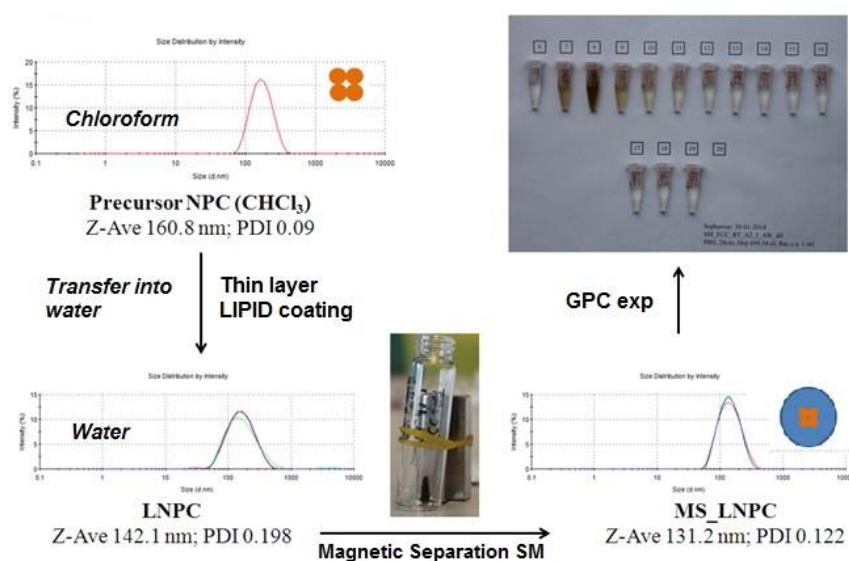


Figure 23. DLS size distributions by intensity; top left LNPs in CHCl_3 ; lower left LNPs in H_2O ; lower right LNPCs following magnetic purification; top right GPC characterization of LNPs.

The chemical and colloidal stability of LNP and LNPC, in MES buffer was confirmed. In addition the MRI properties of the suspensions were assessed to confirm the potential utility of the suspensions as contrast agents for T_1 - and T_2 -weighted MRI modalities, respectively. Finally the absence of cellular toxicity of LNP and LNPC suspensions was confirmed using a wide range of cell types.

5. 2D NPC arrays, optical applications (WP6)

The array formation in the *Level 2* Assembly aims to enable the exploitation of the advantageous properties of the NPCs prepared in previous WPs. This part of the work generally focusses on the preparation of layers, where the specific arrangement of the nanoparticles or nanoparticle clusters allows some functionality or ensures stability. The main activities were grouped around the following core topics:

- i) Large area 2D NPC arrays with high surface coverage.
- ii) Ring-shaped arrays with optical functionalities.
- iii) A micro-characterization platform for thermoelectric NPCs.
- iv) NPC arrays for lighting.

(i) In the first task the preparation of large area ($> \text{cm}^2$) arrays of NPCs with high surface coverage ($>80\%$) has been targeted and achieved. Up to date there is no relevant literature available on the interfacial behaviour of NPCs. The main reason for this is that the preparation of stable and robust NPCs is challenging in itself, and the interfacial assembly represents a rather delicate manipulation

of nanoscale building blocks, where several requirements have to be met simultaneously: physical and chemical stability, proper surface energy to allow trapping at liquid/liquid interfaces.

As a first step, the interfacial assembly method (Figure 24a) was successfully applied and improved for micron sized microparticles. This allowed the preparation of macroscopic samples on the cm scale with high coverage and uniformity (Figure 24b) and was necessary for the anticipated work in (ii) these microparticle monolayers were used as templates for the directed assembly of nanoparticles/NPCs. The interfacial assembly method has been also successfully applied for nanoparticle clusters. The main difficulty of the preparation approach is connected to the presence of the excess ligands in the NPC solution. These excess molecules effectively accumulate at the interface, hindering the NPC in the formation of a compact monolayer. Surface pressure studies performed on the NPC (sub)monolayers allowed us to effectively overcome this difficulty, resulting in high quality NPC monolayers (Figure 24c). While the NPCs for neat monolayer at the interface, they also flatten and deform to some extent (Figure 24d), which is consistent with the non-solid nature of these object, originating in the preparation method of the *Level 1 Assembly*.

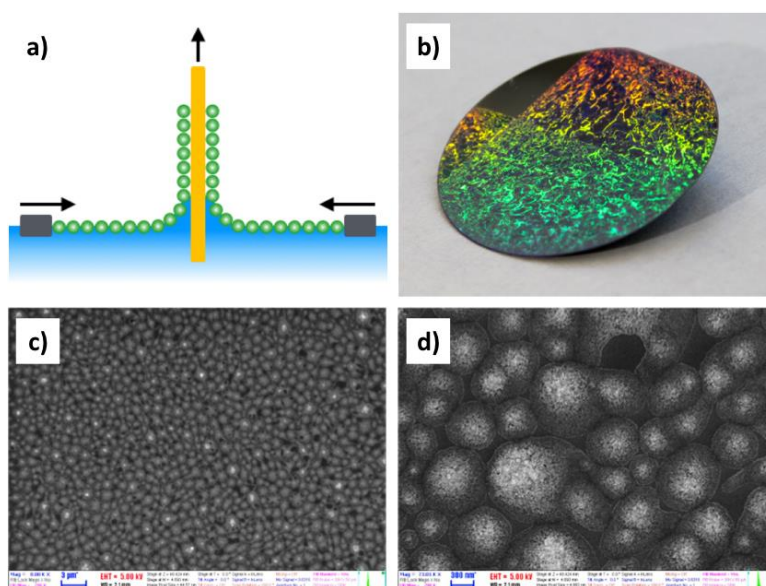


Figure 24: (a) Sample preparation scheme of the interfacial assembly relying on the Langmuir-Blodgett method. (b) Closed array of micron sized particles on a 3" Si wafer prepared for capillary lithography experiments as templates for the assembly. (c) SEM image of a Fe_2O_3 @oleylamine NPC monolayer deposited on Si substrate. The sample shows high uniformity and high coverage. (d) The solid-supported NPCs deform to some extent.

(ii) The preparation of ring shaped arrays with optical functionality were targeted in the second sub-task by the capillary lithography approach. This approach relies on the controlled dewetting of substrates covered by a template structure [Nagy, N.; Zámbo, D.; Pothorszky, S.; Gergely-Fülöp, E.; Deák, A. Identification of Dewetting Stages and Preparation of Single Chain Gold Nanoparticle Rings by Colloidal Lithography. *Langmuir* 2016, 32 (4), 963–971].

The template consists of the polystyrene microparticle monolayer (different particle diameters in the range of 0.6-2.5 microns) shown above. The solution of the nanoparticles or nanoparticle clusters was drop-casted on the monolayer in a controlled way, that is the spreading of the solvent is restricted by a PTFE ring placed directly on the template layer (Figure 25a) and drying of the solvent is performed at constant temperature and humidity. As the solvent evaporates, the liquid film gradually thins until it reaches a critical thickness and macroscopic film rupture takes place. The template monolayer, however, together with the particles or NPCs is still wetted by the liquid. Further evaporation causes the liquid film to break-up and form liquid annuli below the template particles. With the diminishing liquid annuli, the objects become arranged into a circular structure under the action of capillary forces (Figure 25b). Besides capillary, colloidal forces also play a key role in the process. When the template particles and assembled object bare surface charges with

opposite sign, spontaneous deposition at the solid/liquid interface takes place simultaneously (Figure 25c,d) governed by the electric double layer interaction. Nevertheless, this approach truly enables the massively parallel preparation of functional nanostructures. The particle rings e.g. show high SERS activity, this will be reported in an upcoming publication.

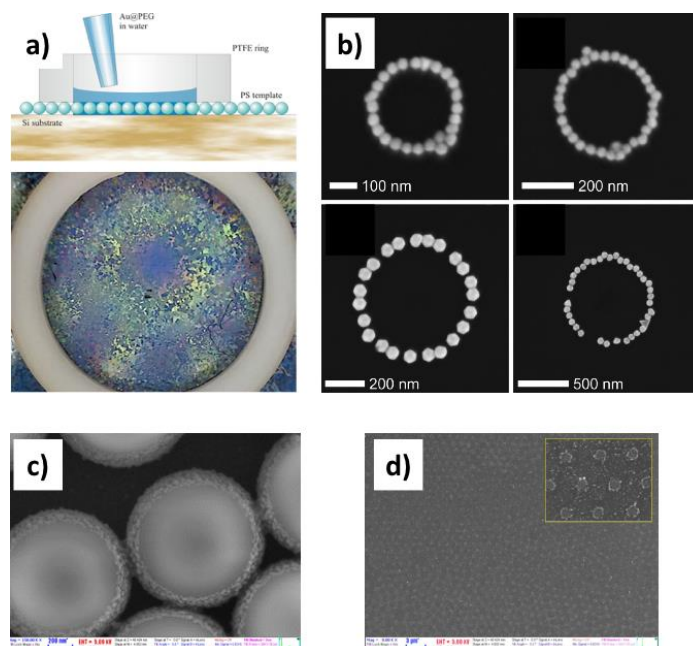


Figure 25: Nanoparticle rings prepared by capillary lithography.

Besides plain nanoparticles and NPCs, branched nanoparticles can also be used for the capillary lithography process. The plasmon resonance of these empty, multibranch gold nanoparticles can be tuned in a wide wavelength range and are excellent candidates for sensing applications [Blanch, A. J.; Döblinger, M.; Rodríguez-Fernández, J. *Simple and Rapid High-Yield Synthesis and Size Sorting of Multibranch Hollow Gold Nanoparticles with Highly Tunable NIR Plasmon Resonances. *Small* 2015, 11 (35), 4550–4559*]. By developing optical simulations on individual multi-branched NPs, their optical properties and near-field distribution could be analyzed. This theoretical data contributed to the evaluation of the Raman Scattering from individual particles and from rings assembled using capillary lithography.

(iii) The micro-characterization platform can be useful for the simultaneous characterisation of thermal and electrical conductivity of objects as small as 1.5 microns. The design principles were based on finite-element calculations, where first possible device structures achievable with micro-fabrication techniques were implemented to simulate the achievable thermal gradient on a hypothetical NPC composed of thermoelectric nanoparticles. Based on the theoretical calculations, the device structure has been implemented. The core of the device is long 1.5 mm wide slit opened is a suspended silicon nitride membrane. This membrane is partly supported by pillars to counterbalance thermal stress but avoid excessive heat transport (Figure 26a). Both sides of the slit are covered by metal, so that electric conductivity and temperature measurements can be carried out simultaneously. Three heating coils connected in serial are integrated on the membrane (Figure 26b). The gap is masked in the regions between the heating elements.

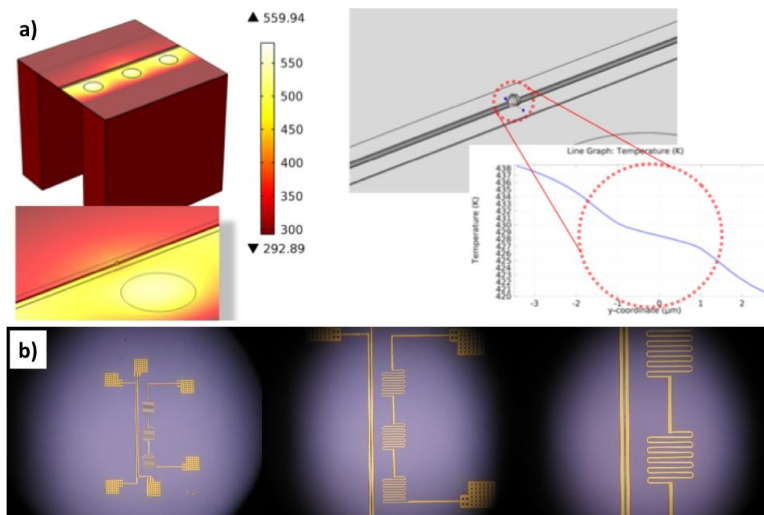


Figure 26: (a) 3D model and corresponding temperature distribution of the device. A microscale NPC at the gap experiences a few K thermal gradient. (b) Optical micrograph of the realized structure.

(iv) The plasmonic near-field modulated emission enhancement could be used to fine-tune the emission properties of metal/fluorescent NPCs. As down converters for white light LEDs, the narrow spectral emission of colour tuneable quantum dots offers selective optical down-conversion of a backlights blue emission into redder light, leading to superior colour rendering index and correlated colour temperatures while maintaining a very high efficacy. Hybrid $\text{CH}_3\text{NH}_3\text{PbX}_3$ and inorganic CsPbX_3 perovskites ($\text{X} = \text{Cl}, \text{Br}, \text{I}$) have very recently emerged as an exceptionally interesting type of new materials, which have huge room for improvement. The emission properties of the combined arrays of plasmonic nanoparticles and perovskites were investigated, Figure 27. Addition of gold had a detrimental effect on the fluorescent properties. Nevertheless, the encapsulation method developed in UNION enabled preparation of a new type of perovskite structure which can be used as a converter layer with promising colour rendering index and superb stability.

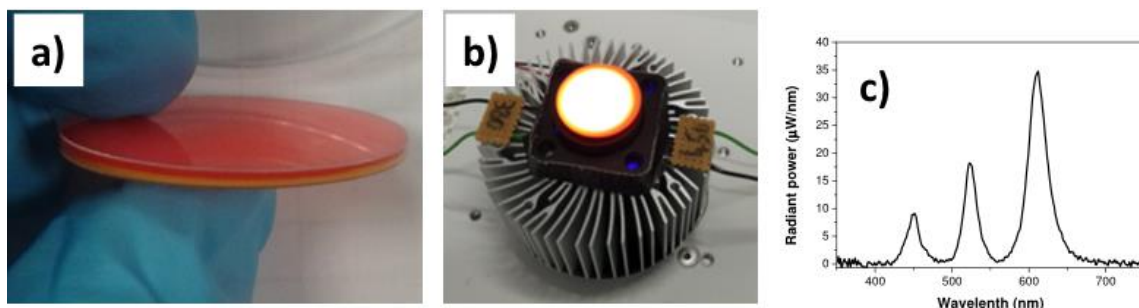


Figure 27: (a) The developed perovskite converter layer with improved stability. (b) The layer produces warm white emission colours when pumped by a commercial high-power blue emitting LED. (c) The emission spectrum clearly shows extremely narrow emission peaks from the perovskites around 520 and 620 nm (blue contribution from the pumping LED).

6. Nanocomposite formation; thermoelectrics (WP7)

Nanomaterials hold the key to produce high efficiency thermoelectric devices well beyond the current state of the art. To achieve this goal, technologies allowing the production of macroscopic 3D nanomaterials with a precise control of material at the nanoscale and having a sufficient material versatility are required. In this direction, within UNION we have developed a versatile and simple bottom up assembly strategy based on the assembly of size, composition and shape controlled colloidal NP building blocks to produce 3D nanomaterials with exceptional parameter control. Following this strategy, we produced semiconductor-metal nanocomposites with thermoelectric figures of merit (ZT) well beyond $\text{ZT} = 1.5$ based on PbS. We used the same strategy to produce Pb- and Te-free nanomaterials with $\text{ZT} > 1.0$, achieving a main goal of the project and particularly of WP7. We further used this strategy to produce a NP-based thermoelectric module. Our results

demonstrate the potential of bottom-up assembly technologies to produce high efficiency thermoelectric materials and to use these materials to produce solution processing devices with state of the art performances.

We detail here the main results in four main directions: i) the control of the doping concentration in NCs by surface treatment; ii) the bottom-up assembly of NPs to produce nanocomposites with thermoelectric figures of merit up to $ZT=1.7$; iii) the assembly of Te- and Pb-free NPs to produce environmental friendly nanocomposites with $ZT=1.2$; iv) the fabrication of a NP-based TE module.

i) *Electronic doping using surface ions* [*Journal of the American Chemical Society* **2015**, *137* (12), 4046-4049]

Halide ions were used to develop a new ligand removal procedure with three goals; (i) removal of organic ligands from the NP surface; (ii) introduction of assembly directors for the formation of NPCs and macroscopic nanocomposites, and; (iii) controlling the charge carrier concentration. As an example, HCl was demonstrated to provide a facile way partial removal of oleic acid (OA) from the surface and at the same time to dope PbS NPs. Chlorine is a common n-type dopant in bulk PbS. We believe that Cl^- remains at the PbS NP surface after OA displacement, and from there it incorporates to the PbS anion sub-lattice during the nanocomposite consolidation step. The displacement of OA by HCl was carried out by injecting controlled amounts of a 1.25 M HCl ethanol solution in 1 g of PbS NPs dissolved in chloroform. The mixture was stirred at room temperature in an argon filled glovebox for 1 h before purification by multiple precipitation/re-dispersion steps using anhydrous chloroform/methanol as a solvent/non-solvent. For HCl of up to 4.5%, PbS NPs remained soluble in relatively nonpolar solvents. TGA (Figure 28) of the PbS NPs treated with different quantities of HCl clearly demonstrated the effectiveness of the HCl treatment for displacing OA from the NPs surface. As a reference, a PbS-0% sample, where OA was displaced using NH_4SCN , was produced. In a typical procedure, 6 mL of a 130 mM NH_4SCN solution in methanol was mixed with 1g of PbS NPs in anhydrous chloroform. NPs were then purified, as above. As in the second strategy, the charge introduced during ligand displacement can be used to assemble NPCs and macroscopic nanocomposites; the direction currently being pursued.

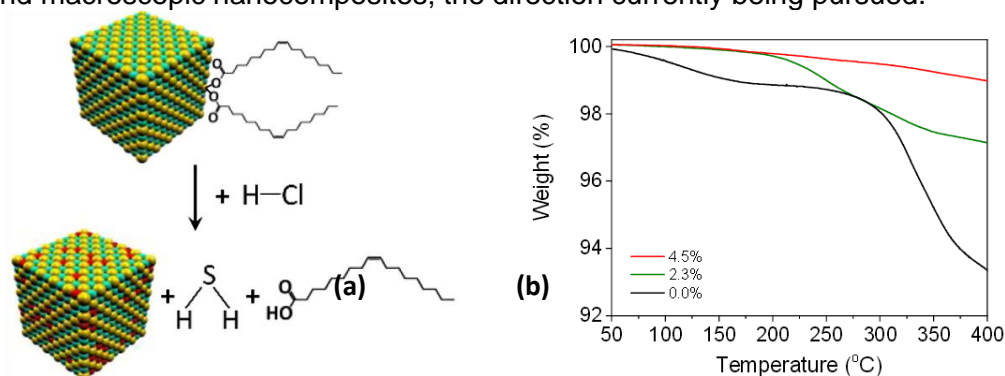


Figure 28. (a) Scheme of the HCl-based doping strategy. (b) Thermogravimetric profiles of HCl treated PbS NPs.

Figure 29 shows the electrical conductivity and Seebeck coefficient of the consolidated nanocrystalline PbS pellets obtained from PbS NPCs obtained by uncontrolled aggregation of PbS NPs with different percentage of HCl (PbS-x% NPs) where $0\% \leq x \leq 4.5\%$. PbS-OA samples (undoped) were characterized by relatively low electrical conductivities. Pellets produced from HCl-treated NPs were characterized by significantly higher electrical conductivities. Moreover, the electrical conductivities increased with the amount of Cl introduced, up to 2.3%. Above this concentration, a decrease of electrical conductivity, associated with the formation of a $PbCl_2$ secondary phase, was observed. All PbS-x% nanomaterial samples showed negative Seebeck coefficients with monotonically decreasing absolute values as expected for increasing degree of n-type doping (Figure 29b).

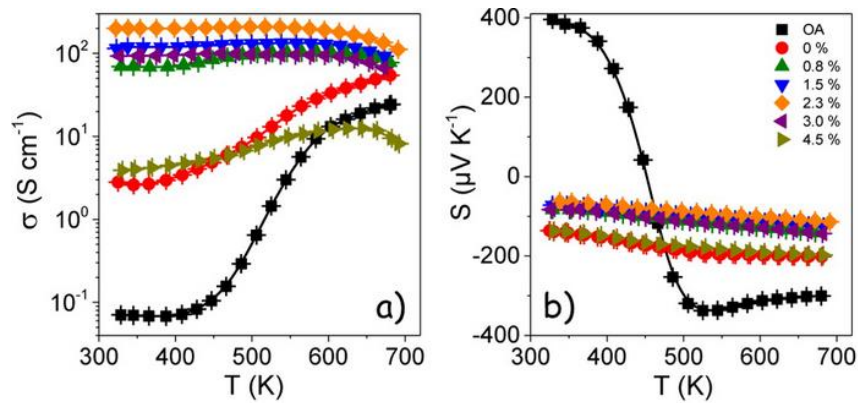


Figure 29 Electrical conductivity (a) and Seebeck coefficient (b) of PbS nanomaterials with different amounts of chlorine NPs.

ii) Bottom-up assembly of NPs to produce high performance thermoelectric nanocomposites [*Nature Communications* 2016 DOI:10.1038/ncomms10766]

PbS-Ag nanocomposites were produced by the hierarchical assembly of PbS cubic NPs and spherical Ag NPs. PbS was selected as the base semiconductor material because of its much lower cost and greater natural abundance compared to tellurium-based semiconductors and because its relatively high figure of merit, $ZT \sim 1.3$ at 923K. On the other hand, as a metallic additive, Ag was chosen owing to its appropriate low work function (4.3 eV), which should allow the injection of electrons into the conduction band of PbS. After hot-press consolidation, PbS-Ag nanocomposites were characterized by a highly homogeneous distribution of metallic Ag nanodomains at the interfaces of a PbS nanocrystalline matrix, as evidenced by high resolution transmission electron microscopy (HR-TEM), high-angle annular dark field (HAADF) scanning transmission electron microscopy (STEM) (Figure 30C, D).

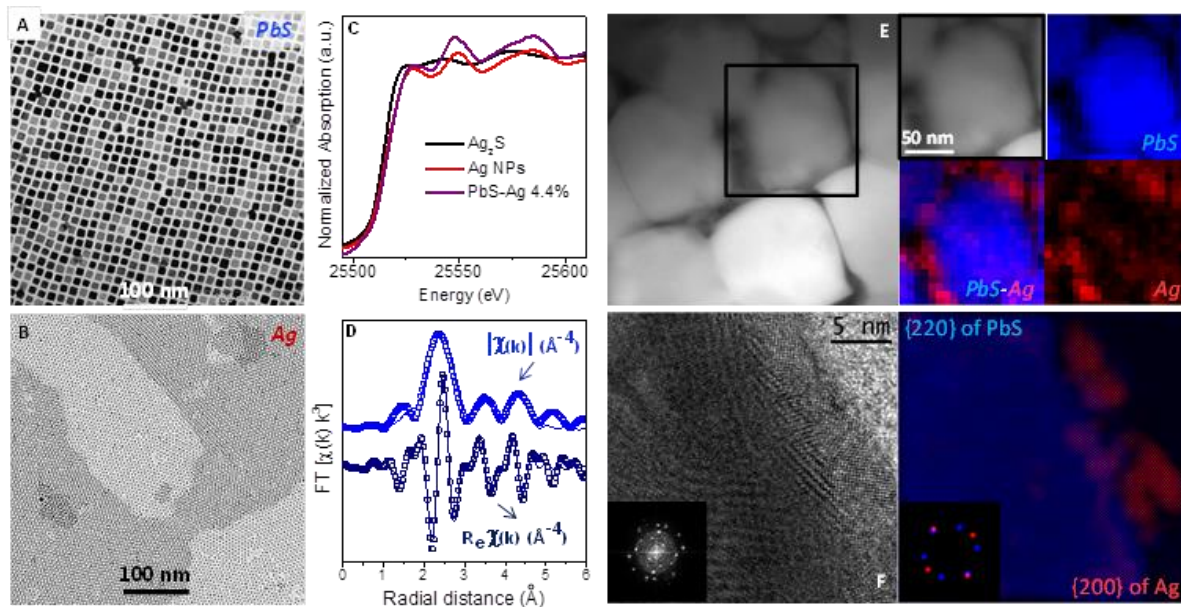


Figure 30. Structural and compositional characterization of initial NCs and resulting PbS-Ag 4.4 mol% nanocomposite. TEM micrographs of (A) PbS and (B) Ag NCs; (C) XAS spectra of the near Ag K-edge of Ag_2S reference (black), Ag NCs (red) and PbS-Ag 4.4 mol% nanocomposite (purple); (D) Fourier transform magnitude, $|\chi(k)|$, and real part, $Re\chi(k)$, of the EXAFS spectrum, the experimental data are given by the dotted line, the best fit by the solid line; (E) HAADF-STEM micrograph and elemental EDX maps; and (F) HRTEM micrograph of the PbS-Ag interface with the corresponding power spectrum (inset) and filtered colorful composite image for the {220} family of planes of PbS (blue) and {200} family of planes of Ag (red). In the filtered images, PbS and Ag are visualized along their [111] and [001] zone axes, respectively.

PbS-Ag nanocomposites presented significantly higher electrical conductivities than bare PbS. At room temperature, electrical conductivities up to 400 S cm^{-1} were measured for the nanocomposites containing a 4.4 mol% Ag (Figure 30A). Additionally, PbS-Ag nanocomposites exhibited negative Seebeck coefficients throughout the temperature range measured. While the absolute value of the Seebeck coefficients decreased with increasing Ag content, the large increase of electrical conductivity compensated for the Seebeck coefficient reduction, and increasingly higher power factors were obtained. The outstanding electrical properties along with the low thermal conductivities resulted in high TE figures of merit of up to $ZT=1.7$ for PbS-Ag (4.4 mol%) nanocomposites at 850 K. This value corresponds to a 40% increase over the highest figure of merit obtained for PbS to date ($\text{Pb}_{0.975}\text{Na}_{0.025}\text{S} + 3\% \text{ CdS}$).

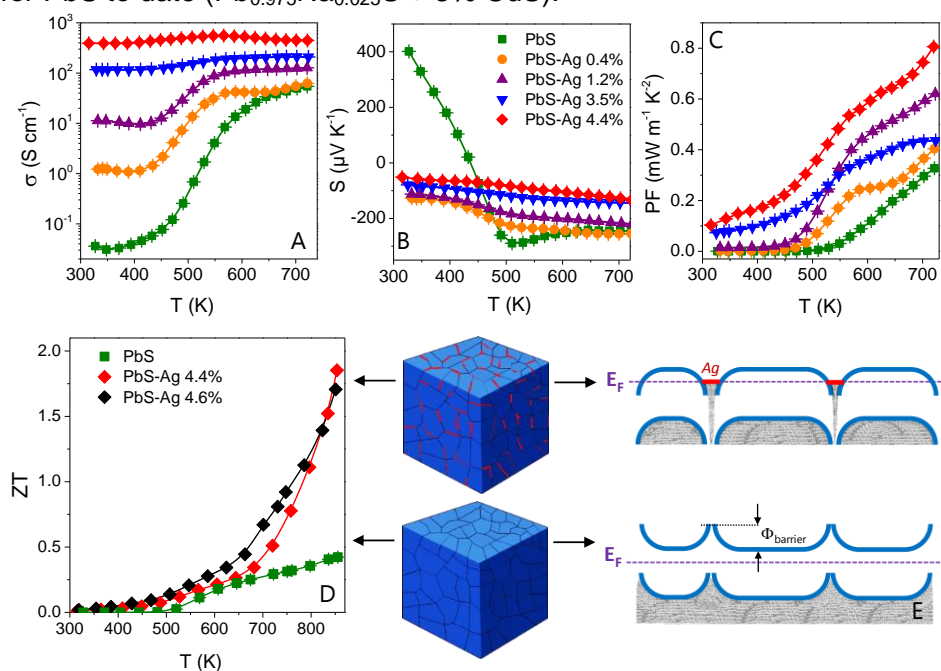


Figure 31. TE properties of x mol% PbS-Ag with $x=0$ (green squares), 0.4 (orange circles), 1.2 (purple triangles up), 3.5 (blue triangles down), 4.4 (red diamonds) and 4.6 (black diamonds). Temperature dependence of the (A) electrical conductivity, σ ; (B) Seebeck coefficient, S ; (C) power factor, PF ; and (D) figure of merit, ZT , up to 850 K. (E) Schematic representation of the relevant band structure differences between undoped PbS and a PbS-Ag nanocomposite.

A nearly endless combination of NPs into nanocomposites still remain to be explored in the effort to optimize charge carrier concentration, maximize the Seebeck coefficient, and reduce thermal conductivity, thereby increasing the overall thermoelectric figure of merit. We are currently exploring in parallel several different material combinations in this direction with the final goal to improve the energy conversion efficiency, of durable, silent and scalable thermoelectric devices.

iii) Assembly of Te- and Pb-free NPs to produce environmental friendly nanocomposites (submitted for publication)

Tetrahedrally coordinated copper-based chalcogenides have recently emerged as an interesting class of functional materials for energy conversion applications, such as photovoltaics, photocatalysis and thermoelectricity. In these fields, the use of nanoparticle-based bottom-up strategies to produce thin films or macroscopic nanostructured materials offer advantages in terms of low-cost processing, improved composition control at the nanoscale and extended surface/interface areas to interact with the media or block phonon transport. However, to optimize material performance, one main standing challenge is the incorporation of controlled amounts of doping within these bottom-up assembled nanostructured materials.

Besides ternary and quaternary Cu-Ga-In, Cu-Zn-Sn, Cu-Ge-Sn chalcogenides, a particularly interesting family of materials that has been scarcely explored is that of I–V–VI tetrahedrally coordinated semiconductors. In particular, Cu_3SbSe_4 (CAsE) is an intrinsic semiconductor with a 0.3 eV direct band gap and a carrier density in the order of 10^{18} cm^{-3} at ambient temperature. It crystallizes in a zinc blende-type tetragonal superstructure that can be viewed as a three-dimensional Cu-Se framework of distorted $[\text{CuSe}_4]$ tetrahedra with inserted one dimensional arrays of $[\text{SbSe}_4]$ tetrahedral. It contains two different Cu positions with different Cu-Se bond length. The valence band maximum is mainly formed by a hybridization of Cu3d and Se-4p states, while the conduction band minimum consists mainly of Sb-5s and Se-4p hybridization. Therefore, the Cu-Se framework provides avenues for charge carrier transport with relatively high mobility, of up to $135 \text{ cm}^2\text{V}^{-1}\text{s}^{-1}$, for un-doped, and of up to $49 \text{ cm}^2\text{V}^{-1}\text{s}^{-1}$ for highly doped, materials. Both copper and antimony atoms are seen to be tetrahedrally coordinated to the bridging selenium atoms. The structure of CAsE shows two inequivalent Cu atoms (Cu1 and Cu2), and each Cu or Sb atom has four Se nearest neighbours (Cu-Se bond length: 2.43 Å and Sb-Se bond length: 2.66 Å). Such rather complex lattice structure is not effective for phonon propagation, what translates in low thermal conductivities. These two properties, combined with an appropriate electronic band structure that includes a large degeneracy at the valence band maximum, makes CAsE an excellent potential thermoelectric material.

However, to maximize semiconductor performance in several fields, including thermoelectric energy conversion, it is strictly necessary to optimize charge carrier concentration. In multinary copper-based chalcogenides with a superlattice structure as that of CAsE, the introduction of dopants in the non-conducting sub-lattice allows doping the material without dramatically decreasing the charge carrier mobility.

Within UNION, we developed the first solution-based scalable synthesis approach to produce grams of monodisperse CAsE NPs with controlled amounts of Sn and/or Bi and used them to produce optimized CAsE nanostructured materials with record TE performances.

The new solution-based large-scale synthesis developed typically yielded more than 2.0 g of $\text{Cu}_3\text{Sb}_{1-x-y}\text{Sn}_x\text{Bi}_y\text{Se}_4$ per batch. Figure 32 shows representative transmission electron microscopy (TEM) and high resolution TEM (HRTEM) micrographs of the $18 \pm 1 \text{ nm}$ CAsE NCs obtained following the previously described procedure. X-ray diffraction (XRD) showed the CAsE NCs structure to be that of a zinc blende body-centred tetragonal phase (I42m) with $a = 5.6609 \text{ Å}$ and $c = 11.280 \text{ Å}$ (Figure 33, JCPDS card No. 85-0003). No secondary phases were detected. Energy dispersive X-ray spectroscopy (EDX) showed that within the experimental error ($\sim 5 \%$) the metal and chalcogenide ratios matched with that of stoichiometric CAsE. After Sn and or Bi doping, the lattice parameters a and c increased, as evidenced by a slight XRD peak shift toward lower angles in Figure 33. The lattice expansion is attributed to the substitution of Sb by larger Sn or Bi ions.

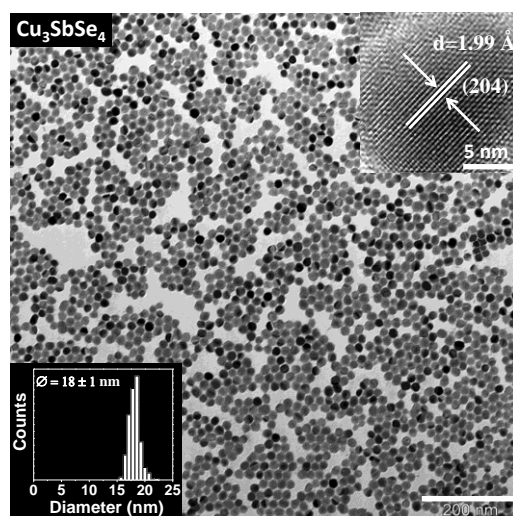


Figure 32. a) Representative TEM micrograph of the CAsE NCs. The inset shows a higher-magnification TEM micrograph; b) HRTEM image of a single CAsE NCs; c) histogram of the measured particle size distribution (18 ± 1 nm).

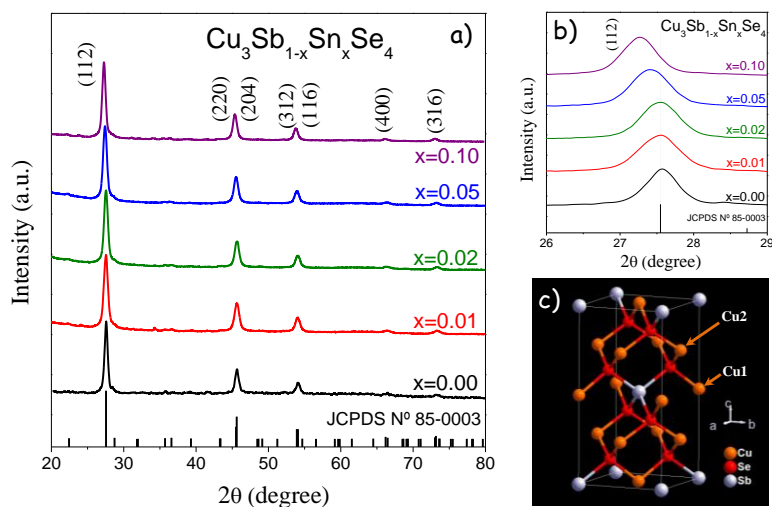


Figure 33. a) XRD pattern of $\text{Cu}_3\text{Sb}_{1-x}\text{Sn}_x\text{Se}_4$ ($x=0.00, 0.01, 0.02, 0.05, 0.10$) NCs. b) detail of the (1 1 2) XRD peak including reference peak data (JCPDS 85-0003). c) unit cell of tetragonal CAsE.

To produce dense and carbon free CAsE nanomaterials, CAsE NCs were thoroughly washed by multiple precipitation/re-dispersion steps, and afterward treated with NH_4SCN to completely displace remaining organic ligands, as confirmed by FTIR analysis. Then, the NC solution was destabilized by increasing its concentration to form NPCs which were subsequently used to produce high density pellets. After solvent removal, the dry NPC-based nano-powder was hot pressed under an Ar atmosphere at 60 MPa at 643-653 K for 30 min into $\text{Ø}10 \text{ mm} \times \sim 1.0 \text{ mm}$ pellets.

The electrical conductivities (σ), Seebeck coefficients (S), thermal conductivities (κ), and the dimensionless thermoelectric figure of merit $ZT = \sigma S^2 T / \kappa$ of $\text{Cu}_3\text{Sb}_{1-x-y}\text{Sn}_x\text{Bi}_y\text{Se}_4$ nanostructured materials are displayed in Figure 34. Un-doped CAsE nanomaterials were characterized by relatively low σ , which increased with temperature up to $6 \times 10^3 \text{ Sm}^{-1}$. Sn-doped materials showed a degenerated semiconductor behaviour and significantly higher σ which increased with the Sn content. The substitution of Sb^{5+} by Sn^{4+} introduces a hole in the structure increasing charge carrier concentration. Remarkably, Sn doping resulted in a dramatic increase of σ , reaching $9 \times 10^4 \text{ Sm}^{-1}$ at room temperature, which is about more than 20 times that of pure CAsE. On the other hand Bi doping slightly decreased electrical conductivity. This may be associated to a decrease of charge carrier mobility with the defect introduction. Additionally, $\text{Cu}_3\text{Sb}_{1-x-y}\text{Sn}_x\text{Bi}_y\text{Se}_4$ exhibited positive S over the entire temperature range measured, which indicated holes as majority charge carries. Pure CAsE shows a high S ($288 \mu\text{V/K}$) at 653 K, which may be attributed to the high hole effective masses. In accordance to the increase of the carrier concentration, the introduction of Sn decreased S . On the contrary, the introduction of Bi had a strong effect on the increase of S associated to a modification of the band structure. When combining both dopants higher power factors were obtained.

Overall, while both dopants Sn and Bi independently helped to increase ZT in single doped materials, the highest ZT values, up to 1.2 were obtained when simultaneously introducing both dopants. Final ZT values are among the highest ever reported for Pb- and Te-free materials in the middle temperature range.

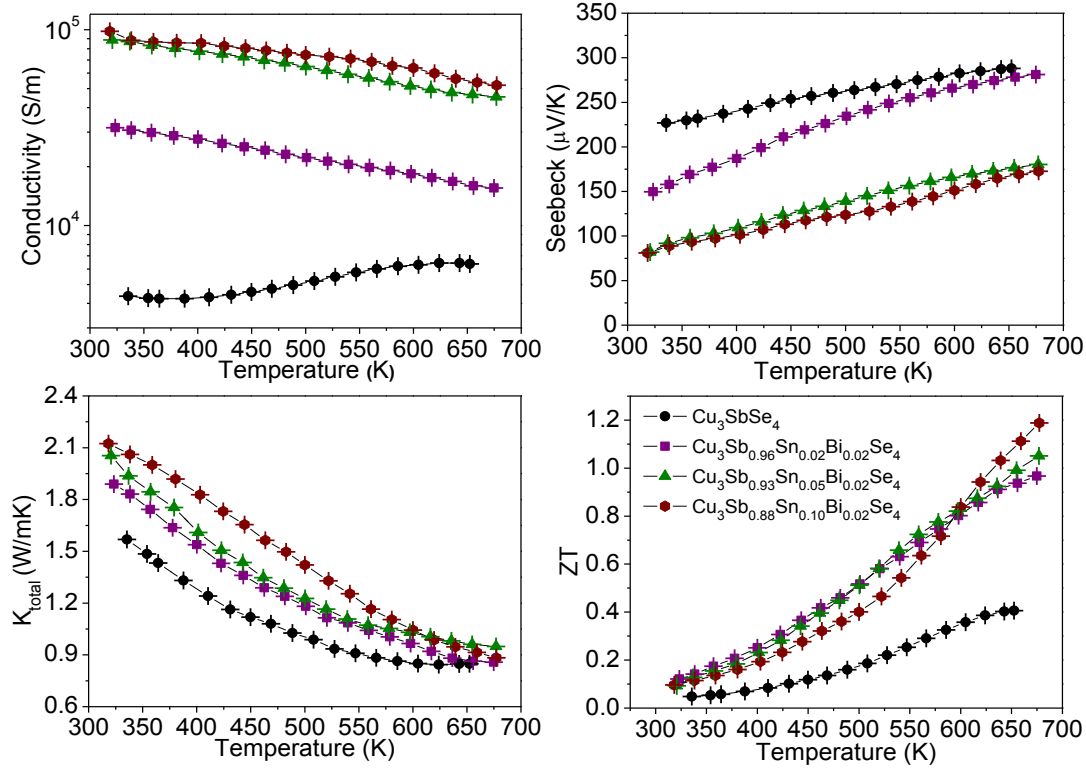


Figure 34. Temperature dependence of (a) electric conductivity (σ), (b) Seebeck coefficient (S), (c) thermal conductivity (κ), and (d) The figure of merit (ZT) of $\text{Cu}_3\text{Sb}_{1-x-y}\text{Sn}_x\text{Bi}_y\text{Se}_4$.

In summary, we were able to produce Te- and Pb- free thermoelectric nanomaterials with ZT up to 1.2 from a 2-step bottom up assembly of colloidal nanoparticles.

iv) NP-based thermoelectric module fabrication

For this task we used a Teflon matrix with holes to maintain the pellets fixed and be able to connect them electrically in series and thermally in parallel and produce in this way a prototype TE module. Polytetrafluoroethylene (PTFE), or commercially Teflon, is a synthetic fluoropolymer easy to work with to obtain the desired layout, electrically insulator and with higher melting point than the temperatures that UNION prototype TE device are intend to reach. We used a matrix with 28 holes, 6 mm diameter, to place the 14 n-p pairs of the final TE device, Figure 35. For the electrical connection between the pellets we used high performance Ag paste. The final device was able to generate a gradient of temperature $\Delta T = 7^\circ\text{C}$ at room temperature when applying 1 V. When working as an energy harvester, was able to generate 10 mV from $\Delta T = 10^\circ\text{C}$.

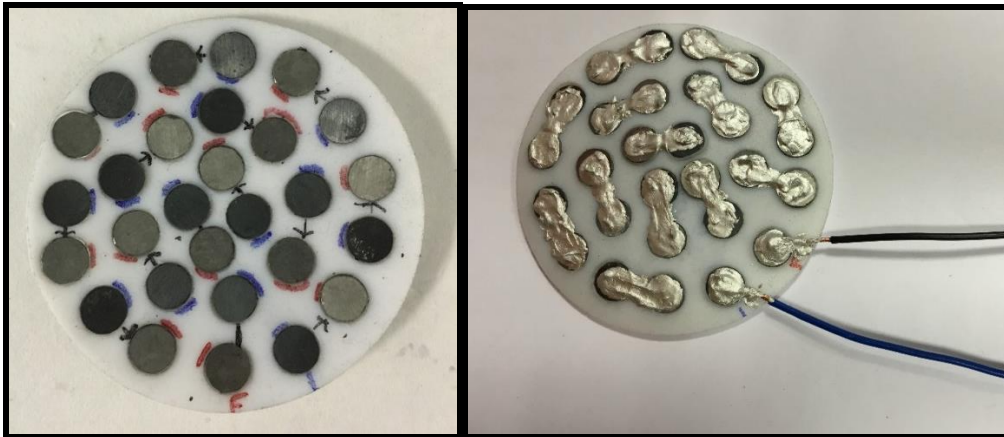
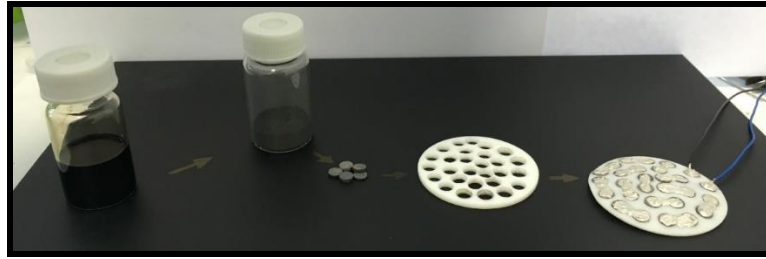


Figure 35: Teflon-based prototype TE module.

(d) Description of the potential impact from UNION

The UNION project was designed to be strongly aligned with the EU vision to invest in research and development projects that will contribute to the transformation of European industry from being resource-intensive to knowledge-intensive. UNION has exploited the potential that nanosciences and nanotechnologies present to produce advances for new energy and material efficient processes.

Specifically, we have applied improved assembly design processes with a view to generating novel high-added-value functional hierarchical nanomaterials.

We have also developed novel in-line monitoring techniques (physical devices) and computational tools that will help develop understanding and control over assembly processes for NPCs and both 2D- and 3D-NPC arrays.

In UNION the magnetic, optical, opto-magnetic and thermoelectric properties of the NPCs, arrays and nanocomposites were characterised to understand how function emerges from the hierarchical order and organized multi-component assembly. This has allowed us to develop new design principles for controlling properties.

As noted above, at the outset UNION our projected outputs included the developing:

- (i) Novel nanomaterials preparation (NPs and NPCs)
- (ii) Understanding NP and NPC formation and properties
- (iii) New materials/applications and their commercial assessment.

In this work UNION has made substantial progress (and some details were provided above). At the end of the project we can summarise our impact under the following headings:

(i) Impact in novel nanomaterials preparation (NPs and NPCs).

In the UNION project we have developed a wide range of NP syntheses and NPC assembly methods, and have improved and scaled-up the syntheses and characterised the materials performance more fully. By combining the expertise across the project we improved reproducibility in NP size, monodispersity and crystallinity for a range of NP types. The development of QC procedures for NPs, which were then rigorously adhered to, allowed us to monitor systematics in assembly properties, from batch-to-batch. This is an example of how progress in nanotechnology could be enabled by the establishment of standards for particle characterisation.

Looking first at NP preparation, in UNION significant efforts were made to optimise the NP synthesis protocols to minimise the environmental impact from health and safety and materials life-cycle perspectives. Two excellent examples of this work are:

- (a) The replacement of toxic cadmium with copper in the preparation of hybrid hierarchical metal-semiconductor Au NR@Cu₂Se nanoparticle assemblies. These were prepared by LMU, by assembly of CdSe NPs on Au NRs followed by cation exchange, producing more environmentally-friendly NPCs with a unique and reversibly tunable plasmonic response. This work was published last year in the Journal of the American Chemical Society: [*“Switching plasmons: gold nanorod–copper chalcogenide core-shell nanoparticle clusters with selectable metal/semiconductor NIR plasmon resonances” Rodríguez-Fernández et al., JACS 2015, 137, 11666.*](#)

- (b) The synthesis of selected high-quality plasmonic, and in particular thermoelectric, NPs were conveniently scaled-up, into the gram-scale, as is required for TE applications. This was achieved without compromising the quality (size, size dispersity, and crystallinity of the nanocrystals. e.g. *“Simple and rapid high yield synthesis and size sorting of multi-branched hollow gold nanoparticles with highly-tunable NIR plasmon resonances”*, Rodríguez-Fernández et al. *Small*, 2015, 11, 4550.

The demonstration of successful scale-up of a range of environmentally friendly NP building blocks was a significant, and critical, contribution for the envisaged UNION work on assembly and the planned applications. For nanotechnology in general, increasing the breadth and quality of NP synthesis, will also contribute to many other applications.

Finally, the consortium made significant strides in developing NPs that are suitable for further assembly into clusters, NPCs. One key issue was found to be the surface ligand (assembly director) coverage; great care was taken to fully disperse NPs (of all types) in suspension. For NP preparation approaches where coverage could be fully controlled it was found that it was possible to reproduce the kinetics of assembly from batch to batch of NPs. This is both an obvious and a profound observation, it was discussed in detail in our recent article, *Nanoparticle Clusters: Assembly and Control Over Internal Order, Current Capabilities, and Future Potential*, Stolarczyk, Deak and Brougham” DOI: 10.1002/adma.201505350.

Turing then to NP assembly into functional NPCs, in UNION we applied a few selected assembly methods to a wide range of NP types, to generate both single- and multi-component NPCs. This established general routes to nanostructures (in suspension) with compositional hierarchy. Subsequently, by studying these assemblies we will investigate the extent of internal order within the compositional hierarchies from each method; how they depend on the thermodynamic driving force for assembly, and on the AD type. There have been numerous publications (described above), but the UNION research included:

- Electrostatic Assembly (ESA) was applied to magnetic NPs, resulting in NPCs with interesting hyperthermic properties, and for assembly of TE NPs at scale. ESA was also used to prepare metal-semiconductor hierarchical clusters of Au NR@Cu₂Se, by assembly of CdSe NPs on Au NRs followed by cation exchange, producing more environmentally-friendly NPCs with a unique and reversibly tunable plasmonic response.
- Polymer mediated assembly (PMA), in both the interface free and micellar collapse forms, was used to prepare NPCs from; (i) spherical and cubic magnetic (γ -Fe₂O₃) NPs, and; (ii) PbS (single NP component), PbS and PbSe (binary TE NP combinations).
- Competitive stabiliser desorption methods (CSD) were used to prepare single and multiple component monodisperse NPCs from γ -Fe₂O₃, CoFe₂O₄, MnFe₂O₄, and TiO₂ NPs reproducibly and at scale.

(ii) Impact in understanding NP and NPC formation and properties

By undertaking this activity the UNION partners have made significant scientific impact by developing understanding of key processes at the nano-scale. For instance:

- IREC and collaborators developed a simple and versatile bottom-up strategy based on the assembly of colloidal nanocrystals to produce consolidated yet nanostructured thermoelectric materials with improved performance. For instance, for the PbS–Ag system, Ag nanodomains contribute to block phonon propagation, reducing thermal conductivity, and also provide electrons to the PbS host semiconductor and reduce the PbS inter-grain energy barriers for charge transport, increasing electrical conductivity. Thus, PbS–Ag nanocomposites exhibit reduced thermal conductivities and higher charge carrier concentrations and mobilities than PbS nanomaterial. This work was recently published; "*High-performance thermoelectric nanocomposites from nanocrystal building blocks* Kovalenko, Cabot et al. *Nature Communications*, 2016, 7, 10766". The manuscript highlights the fact that the relatively facile bottom-up approach opens the way to a nearly endless variety of nanocomposites; these are suitable for high-throughput screening to optimise the TE conversion efficiency of robust, scalable thermoelectric devices.

-DCU, MFA and LMU were invited to review the current state of the art in the use of colloidal methods to form NPCs. The manuscript "*Nanoparticle Clusters: Assembly and Control Over Internal Order, Current Capabilities, and Future Potential*, Stolarczyk, Deak and Brougham" *Advanced Materials*, 2016, DOI: 10.1002/adma.201505350. In it we focused on the two-step approach (as in UNION) which exploits the advantages of bottom-up wet chemical NP synthesis procedures, with subsequent colloidal destabilization to trigger assembly in a controlled manner. The role of NP–NP interactions in the formation of monodisperse ordered clusters was pinpointed and the different assembly processes from a wide range of literature were classified according to the nature of the perturbation from the initial state. In particular the factors limiting the general applicability of colloidal assembly methods, and how these might be ameliorated, were identified. These include; (i) high sensitivity to the initial conditions, and in particular the ligand surface coverage, alters the kinetics and outcome of the assembly process rendering reproducibility difficult, (ii) difficulty in scaling-up the process, for reasons relating to primary NP yield, matter transport at larger volumes, and the presence of competing processes

- DCU and LMU have identified the key conditions that determine size control in thermal decomposition syntheses of magnetic iron-oxide NPs. This is an important area, with the original papers receiving >3000 citations in 10 years. The insights derive from application of accepted kinetic models, and provide clarity to the wide range of seemingly disparate published reports/observations. This work is now in preparation for publication at the ACS.

Furthermore, the effect of internal NPC structure/hierarchy on emergent NPC properties was studied:

- DCU and Nanovector applied a number of NP assembly methods to study the effect of magnetic processing on lipido-magnetic NPCs. Specifically, we determined the effect of internal γ -Fe₂O₃ NP order (NP density and alignment) within the NPCs on the magnetic resonance and hyperthermic efficiencies of NPCs of the same size. This work is currently under review.

- Turning to 2D NPC arrays, MFA identified that preparation it is possible to assemble clean nanocomposite 2D rings composed of a chains of nanoparticles. In the case of gold NPs (above c.40 nm) these structures show strongly localized coupled plasmon mode in the visible part of the spectrum, that could be effectively used in surface enhanced RAMAN spectroscopy (SERS), as compared to single particles or other NP-belt structures reported earlier in the literature.

(iii) Impact in developing new materials/applications and their commercial assessment.

The main objectives were to develop lipido-magnetic NPCs (DCU and Nanovector), nanostructured TE materials (IREC, Cidete and TRT) and process monitoring technologies (Malvern). At the end of the three year project the partners have made significant progress scientifically and towards each of the identified applications. We are now in a good position to develop these applications; towards alpha and the beta testing (for the assembly monitoring technologies), towards further patenting and sourcing in vivo testing (lipido-magnetic assemblies for bio-applications), and towards achieving a higher TRL (thermoelectrics – avionics).

At the end of the three year project the partners have made significant progress scientifically and towards each of the identified applications. This is in part because the commercial potential of selected technologies and materials were assessed during UNION project. This work involved detailed evaluation of (i) performance; (ii) commercial potential, and where applicable; (iii) cost of production; (iv) environmental health and safety implications of production; (iii) life cycle analysis of production; (iv) scale-up possibilities. Roadmaps for the development of each of the technologies/materials in the post-UNION period have been developed. While we cannot provide details of the outcomes of the analysis/planning here, we can outline some of the progress:

For the **assembly monitoring technologies**, nanoparticle and macromolecular characterisation is an important and growing sector of the overall particle characterisation instrument market, and the impact of any developments in this field will help boost growth of the sector. UNION will help develop the current generation of dynamic light scattering systems to incorporate:

- Monitoring of dynamic (i.e. non-equilibrium) suspensions to investigate assembly on different scales and a different levels of scale-up.
- Analysing anisotropic and heterogeneous NPs and NPCs in suspension.

The impact of these innovations will be felt beyond the fields of application within UNION, i.e. across colloidal and protein science and technology; e.g. for in-line process monitoring in bio-fermentation and protein extraction, as well as for emulsion-based processes. UNION partners hope to develop these technologies for a range of applications and in the future potentially incorporate them into their product range. We are currently working towards alpha and the beta testing. These next steps will be completed in house and with partner laboratories, using available resources.

Considering the development of **lipido-magnetic nanomaterials** as MRI-trackable delivery vehicles; although much has been published on advantages of proprietary nano-carriers for drug delivery application, clinical development has not yet started as standardization of production and monodispersity of size and drug loading of even single NPs has yet to be achieved. These requirements map directly onto the UNION objectives, wherein the partners have developed a

deeper understanding of the microemulsion process for coating and for the formation of lipid NPs. The UNION partners have shown that it is possible to prepare NP and/or NPC suspensions using thin lipid stabilizing layers and that it is possible to load the outer layers of LNPs or LNPs with model drugs. There are no identified EHS or LCA issues associated with the production of LNP or LNPC suspensions, they exhibit no cellular toxicity and the cost of production is not a significant barrier. Theranostic products (dual delivery and diagnostics) are expected to bring real innovation in medicine: the development of magneto-lipidic NPCs within UNION provides a solution of a bio-compatible MRI-trackable delivery vehicle for image guided therapy and/or stimulated release. The technologies developed by UNION are ideal for the delivery of a wide range of hydrophobic moieties, which must be properly formulated in a nano-carrier, for use in man. Hence UNION technologies are anticipated to be of interest to the big pharma companies. The next steps will involve consideration of IP protection, identification of other sources of national project funding (this is underway) and eventually of industry partners with appropriate laboratory facilities for in vivo testing. Those contacts are being made.

Turning to **nanostructured materials for thermoelectric applications**; the concept of generating clean power from waste heat is alluring and is gaining significant attention worldwide. Given that nearly 60% of the world's fossil-fuel energy is wasted as heat, if even a fraction of this heat could be converted to useful electric power, both energy efficiency and sustainability would be dramatically increased. Efficient thermoelectric materials have a huge potential to develop competitive products in a wide range of application fields. BASF estimated the thermoelectric market in 2003 to be M€160. Today, the Fraunhofer Institute estimates the market to be already over M€500, and that a ZT of 2 would multiply the market volume by a factor 10. Enabling thermoelectric modules to enter into such markets would have tremendous economic, industrial, environmental and societal impacts. Thermoelectricity is a promising technology for which exploitation demands improved materials; and nano-structuring of TE materials offers the most likely route to improved efficiency, in particular for energy harvesting for autonomous sensors and systems. Highlighting just a couple of market applications, micro power (for example, powering remote sensors or other portable applications) is eminently feasible with current technology. Furthermore, the market for remote power is undeniably large. Sensors alone represent a total available market of 8 billion units by 2012. While only a portion of this market will benefit from remote power, a reasonable estimate puts the ultimate potential at over 100 million units per year, for this application.

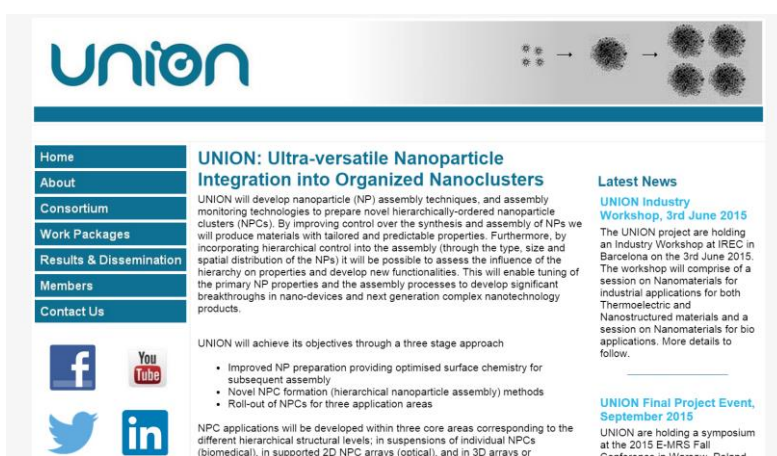
In UNION a promising material was selected by partners and a final TE device was able to generate a significant temperature gradient at room temperature when applying a low voltage and similarly to develop a usable voltage with a moderate temperature gradient. A general specification was developed including environment constraints, general specifications, test procedures and thermal performances specifications. The selected nano-material was then assessed with respect to the requirements of a particular electronics application. The results demonstrated that the UNION nanomaterials offer an interesting alternative to commercial materials which partially meet stringent specifications. We have concluded that UNION nanomaterials may represent a future alternative to current TE materials due, in particular, to their sustainability and their scalable and potentially very stable production process. Further studies will have to be conducted through collaborative research projects integrating actors from the industrial supply chain, in order for the identified technical solution to increase in technology readiness level.

The selected application was in avionics electronics, a major area of interest for the UNION partner TRT, as it would allow for a reduction in equipment weight with downstream cost- and environmental-benefits. The expected financial impact of TE technology in this area arises through the planned next-generation avionics systems which will incorporate “*Integrated Modular Architecture*” (IMA). TRT foresees the UNION platform as a key enabling technology for the new generation of aircraft. It is predicted that each new medium to large aircraft (commercial aircraft, business, regional jets, and helicopters), designed in the early 21st century will use the IMA concept. Advanced packaging and cooling solutions would participate in maintaining or gaining market share. In the shorter term, for the applications identified by TRT; higher TRL studies are envisaged through collaborative research projects integrating future supply chain actors. Additional partners are being sought to provide relevant end-user skills. A decision on how that work will be funded; be it through the resources of partners, or through external research funding, is currently under consideration.

4.2 Use and dissemination of foreground

(i) Dissemination Activity During the project

The **UNION website** (<http://www.fp7-union.eu/>) constituted the main dissemination channel for the project. It has been maintained and updated throughout the project, with the most useful sections for dissemination purposes Results & Dissemination and Latest News, which have been updated with every new or output of the project. In addition, the private section of the project website has been a major tool for sample tracking, monitoring joint work, and time planning. A video and a poster presentation of UNION were prepared at the beginning of the project and made available to the partners to facilitate external dissemination.



The **UNION scientific results are already being published** with 24 peer reviewed papers in international high impact journals (including *Nature Communications*, *ACS Nano*, *Small*, *JACS*, *Advanced Materials*) to date, and with many more under review or in preparation. UNION partners have delivered 33 invited lectures, 35 oral presentations and 18 poster presentations at major international conferences around the world (MRS, E-MRS, International and European Conference on Thermoelectrics, NANAX 6, EuroNanoForum, etc). The complete list of dissemination activities can be found on the Results & Dissemination section of UNION website. <http://www.fp7-union.eu/results%20and%20dissemination.html>



The **thematic UNION Newsletters** have been used to promote dissemination of UNION results and technologies. Each newsletter (winter 2013/14 <http://eepurl.com/R-YX9>, summer 2015 http://eepurl.com/btQ_H9, and winter 2015/16 <http://eepurl.com/bN1Lg9>) focused on a different topic from the project, and paid special attention advertisement of the upcoming dissemination and exploitation events, e.g. the Industry Workshops.



UNION held its **Final Project Event at the E-MRS Fall Meeting** in Warsaw, Poland in September 2015. We organized Symposium M *“Hierarchical Assembly of Nano-Scale Building Blocks”* <http://www.european-mrs.com/2015-fall-symposium-m-european-materials-research-society>. The event, held together with 22 parallel symposia, ran over three days and was divided into 12 sessions. Close to 100 abstracts were received and there were over 200 registered attendees. A selection of hot topics in the field of nanoparticle assembly were included in the presentations, these were given by prominent invited speakers and UNION researchers.

- Mechanisms and strategies for the preparation of nanoparticle clusters and 1D, 2D and 3D nanoparticle assemblies.
- Modelling of nanoparticle self- and directed-assembly
- In-situ characterization of nanoparticle assembling
- characterization of nanoparticle assemblies
- Modelling optical and transport properties of nanoparticles assemblies
- Use and integration of nanoparticle assemblies in biomedical, energy conversion and storage, optoelectronic, photonic, and other relevant applications
- Scale-up of nanoparticle synthesis and assembly processes



The **UNION Industry Workshops** were organised to promote industry collaboration and facilitate future market entry for our technologies. UNION organised two workshops, targeted at the UNION application market sectors, which were held in Barcelona, Spain, in June 2015. The location was chosen due to the large number of industries, SMEs and start-ups in the relevant sectors in Catalonia. The goals of the workshops were to:

- Showcase the UNION technologies
- Identify the current technological challenges/opportunities in nano-structured materials (TE and bio) and explore possible approaches to these
- Establish new alliances and collaborations (both using current resources and via Horizon2020 and National funding); with a view towards industrial exploitation and discussion of possible licensing agreements.

The Thermoelectrics Workshop “Nanomaterials for industrial applications” included sessions on “Thermoelectric Materials” and “Nanostructured Materials”. The Bio Workshop “Nanomaterials for bio-applications” included sessions on “Soft Materials / therapy / Regulatory” and “Diagnostics”. In addition, we scheduled an “Exhibition of manufacturing equipment and measurement units”, with inputs from both TE- and Bio-industries. We had 25 presenters from a total of 41 attendees, representing 18 industries (excepting the UNION partners).



Arising directly from the workshops the UNION partners have initiated new collaborations, and have identified partners for national and H2020 funded programmes. We anticipate that those funding

bids will be competitive as we now have a clearer view of the current activity, challenges and unmet needs in the two application fields of interest.

Our exploitation activity was enabled by an Exploitation Strategy Seminar (ESS) during the project meeting in Feb 2014 (Paris), provided by an external facilitator appointed by the EC. The main exploitable results of each partner were identified, and the need for clarification of foreground IP (in particular) was identified, the main outcomes are listed in the Tables 4..2 below. Subsequently UNION has prepared three roadmaps plotting further development of the different technologies for their industrial deployment: assembly monitoring techniques, thin lipid layer technology (bio-application) and thermoelectric materials and devices.